"STRESS ANALYSIS OF A PIPING SYSTEM"

A Dissertation

Submitted in Partial Fulfillment of the Requirements

of

MASTER OF TECHNOLOGY
IN
MECHANICAL ENGINEERING
(CAD/CAM)

By

Surendra Kumar Meghani

Under the guidance of

Prof. D. S. Sharma
Mr. N.V. Prakash

Department of Mechanical Engineering

INSTITUTE OF TECHNOLOGY

NIRMA UNIVERSITY OF SCIENCE & TECHNOLOGY,

AHMEDABAD 382 481

JUNE 2006

Certificate

This is to certify that the Major Project Report entitled "**Stress Analysis of A Piping System**" submitted by **Mr. Surendra Kumar Meghani (03MME007)** towards the partial fulfillment of the requirements for the Master of Technology (Mechanical) in the field of **(CAD/CAM)** of **Nirma University of Science and Technology** is the record of work carried out by him under our supervision and guidance. The work submitted has in our opinion reached a level required for being accepted for examination. The results embodied in this major project work to the best of our knowledge have not been submitted to any other University or Institution for award of any degree or diploma.

Date:

Prof. D.S. Sharma
Guide (institute)
Professor, Mechanical Engineering Department, Institute of Technology, Nirma University, Ahmedabad.

Prof. A.B. Patel
Head of Mechanical Engineering Department, Institute of Technology, Nirma University, Ahmedabad

Mr. N.V. Prakash
Guide (industrial),
Manager, Technical,
Intergraph Consulting,
Hyderabad.

Dr. H.V.Trivedi
Director,
Institute of Technology,
Nirma University, Ahmedabad.

Examiners:

1)……. 2)…….

3)……. 4)…….

Acknowledgement

I would like to begin by expressing my thanks to both of my guide Prof. D.S. Sharma and Mr. N.V. Prakash. Their encouragement and unfailing support have been most valuable to me during these periods, and I feel deeply privileged for the opportunity to work with them. Their guidance as a guide, mentor and friend is greatly appreciated.

I would also like to express my gratitude to my Head of the Mechanical Engineering Department, Prof. A.B. Patel, for their advice and help during the entire duration of the project work.

I would also like to express my gratitude to Mr. Kancherla Umamaheshwara Rao (Divisional Manager, PPM, Intergraph Consulting), Mr. Nidugondi Ravishekhar V. (Manager, Technical, PPM, Intergraph Consulting) & Mr. K.K. Meghani (Manager, Development, PPM, Intergraph Consulting) for providing me their valuable guidance to me throughout the dissertation.

I am also heartily thankful to review committee member Prof. D.S. Sharma, Prof. K.M. Patel & Prof. B.A. Modi, for their suggestions, critics and the clarity of the concepts that helped me a lot during this study.

I am also thankful to all the faculty members of mechanical engineering department for helping me directly and indirectly.

Finally, I would like to express my gratitude to Intergraph Consulting, Hyderabad for providing me the golden opportunity to carry out this dissertation work there and for providing high performance computing resources and support for my dissertation.

Surendra Kumar Meghani
03MME007
M.Tech. (CAD/CAM)

Abstract

The study under this thesis work covers the static, thermal and transient flow analysis of a piping system used in a leading pharmaceutical company for making an anti-hypertension drug. The piping system under study was modeled in the commercial piping software, CAEPIPE. The study considers the static, thermal and dynamic stresses due to water hammer effect. In the static analysis, the stresses, displacements, support forces and moments and element forces and moments were obtained. Results obtained from the software show that the piping system is safe in static analysis. In the thermal analysis also the stresses, displacements, support forces and moments and element forces and moments were obtained. The results of thermal analysis show that system was getting failed due to excessive thermal stresses at various nodes. For solving this problem, some modification in the model were done by removing and relocating some of the supports or restraints. And comparisons were made between the results of original and modified model for stresses, displacements, element forces and support forces and moments. In the water hammer analysis of the piping system, dynamic stresses were found out for the closing of different valves separately. Also the valve closure times for the valves and the reflection periods of the different sections were found out. Graphs were obtained for pressure variation with the valve closure times for the valves. The results show that the system is under no threat due to the water hammer effect.

List of Figures

List of tables

Nomenclature

I	:	Moment of inertia of pipe cross section
I_i	:	In-plane Stress Intensification Factor
I_o	:	Out-plane Stress Intensification Factor
Mi	:	In Plane moment
Mo	:	Out of plane moment
P	:	Pressure
Pa	:	Axial force from internal pressure
S_H	:	Hoop Stress
S_L	:	Longitudinal Stress
T_1	:	Temperature
t	:	Pipe wall thickness
d_i	:	Pipe inner diameter
A_m	:	Cross sectional area of pipe
d_o	:	Outer diameter of the pipe
F_L	:	Axial force
M_b	:	Bending moment
y	:	Distance from the neutral axis of the pipe
M_T	:	Torsional moment
R_T	:	Torsional resistance
$S_{allowable}$	:	Allowable expansion stress
S_h	:	Basic allowable stress at maximum metal temperature during the displacement cycle under analysis
S_c	:	Basic allowable stress at minimum metal temperature during the displacement cycle under analysis
S_A	:	Allowable expansion stress range

S_E : Displacement stress range

Z : Section modulus of pipe

St : Torsional stress

S_b : Resultant bending stress

h : Flexibility characteristic

k : Flexibility factor

R_1 : Bend radius of pipe

r_2 : Mean radius of pipe

$\overline{T}$: Pipe fitting thickness

OPE : Operating load case

SUS : Sustained load case

EXP : Expansion load case

f : Stress range reduction factor for displacement cycle conditions for the total number of cycles over the expected life.

Contents

Chapter 1

Introduction

1.1 Introduction

Stress analysis is a subject, which is more talked about and less understood. Piping stress analysis is a term applied to calculations, which address the static and dynamic loading resulting from the effects of gravity, temperature changes, internal and external pressures, change in fluid flow rate and seismic activity. Codes and standards establish the minimum requirements of stress analysis. The objective of the stress analysis is to ensure safety against failure of the piping system by verifying the structural integrity against the loading conditions, both external and internal, expected to occur during the lifetime of the system in the plant. The analysis ensures that the piping system meets intended service and loading conditions requirements.

The load cases for the purpose of analysis of piping system are as follows:

1. L1 = W+T1+P1 (OPE)
2. L2 = W+P1 (SUS)
3. L3 = T1 (EXP)

While doing analysis of the piping system, besides checking nodal loads or restraint loads, code stresses should also be checked. If percentage of code stress check is higher than 100% i.e. the ratio of maximum stress/allowable stress is more than 1, then the system will fail, whatever may be the nodal or restraint loads. For stress check, load cases L2 and L3 should be selected and for displacements and load check, load cases L1 and L2 should be selected.

Changes in temperature affect all dimensions in the same way. In this case thermal strain is handled as strain due to an applied load. For example, if a bar is heated but is constrained the stress can be calculated from the thermal strain and Hook's law.

$$\sigma_{th} = E\varepsilon_{th}$$

Where E is the modulus of elasticity and ε_{th} is the thermal strain, the length L, area A, and volume V, strain are calculated with the following equations:

$$\Delta L = \alpha L_0 (T_2 - T_1)$$

$$\Delta A = \gamma A_0 (T_2 - T_1)$$

$$\gamma \approx 2\alpha$$

$$\Delta V = \beta V_0 (T_2 - T_1)$$

$$\beta \approx 3\alpha$$

In the thermal analysis, the effect of temperature on the piping system has been studied. A pipe may experience expansion or contraction once it is subjected to temperatures higher or lower respectively as compared to the temperature at which it was assembled. Due to temperature gradient, expansion and contraction of pipe takes place, which will result in to displacement of system. The maximum and minimum displacements due to these temperature gradients must be within allowable limits. Thermal analysis gives the results in the form of expansion stresses, stress ratios at all the nodes of the piping system. It also gives the forces and moments on the anchors and restraints and element forces as well. The positions of the supports also affect the expansion stress distribution in the piping system. The model has been subjected to different positions of the restraints and supports for the purpose of analyzing the effect on the stress distribution.

The stress intensification factor (SIF) is defined as the ratio of the maximum stress intensity to the nominal stress, calculated by the ordinary formulas of mechanics. It is used as a safety factor to account for the effect of localized stresses on piping under a repetitive loading. In piping design, this factor is applied to welds, fittings, branch connections, and other piping components where stress concentrations and possible

fatigue failure might occur. The SIF affects the expansion stresses in the bend. Due to the circumferential stresses the bend or elbow is subjected to repeated in plane bending and develops a fatigue crack. These circumferential stresses are taken care by multiplying the stresses at the bends due to bending moment by SIF. Static stress analysis finds the stresses as per the governing equations given by the ASME B31.3. The code stresses are found out and then compared with the allowable limits. The displacements, forces and moments on the supports and restraints can also be found out.

The effect of suddenly stopping or accelerating a fluid by closing and opening a valve may induce a water hammer overpressure. If this overpressure is enough the pipeline may fail or deform. Water hammer normally occurs during the opening or closing of valves, and it generates an acoustic wave that propagates upstream and downstream of the system. Figure 1.1 shows a diagram illustrating this phenomenon. This transient phenomenon manifest as a big noise coming out of the pipe. This is what is heard sometimes when the water faucet is suddenly open or close.

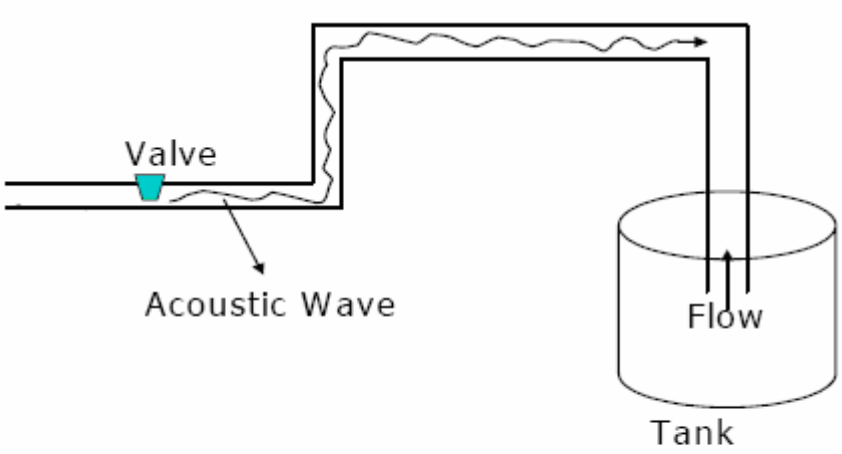

Figure 1.1: Acoustic wave in pipes

There are four phases in which the pressure wave generally travels in the piping system during water hammer phenomenon. The first phase occurs after the valve has closed but

before the resulting wave has traveled the pipe length and reached the upstream reservoir (see Figure 1.2, Phase A). The second phase occurs after the wave has reflected from the inlet reservoir but before it has come back to the valve. The wave, still moving at speed a, travels from the reservoir to the valve (see Figure 1.2, Phase B). The third phase occurs after the wave has reflected from the inlet reservoir, traveled back to the valve and reflected from the valve, and is now moving back towards the reservoir (see Figure 1.2, Phase C). The fourth phase occurs after the wave has reflected from the inlet reservoir for the second time and is moving back towards the valve (see Figure 1.2, Phase D). These four phases are shown in the following figures along with the pressure and velocity variation during the travel:

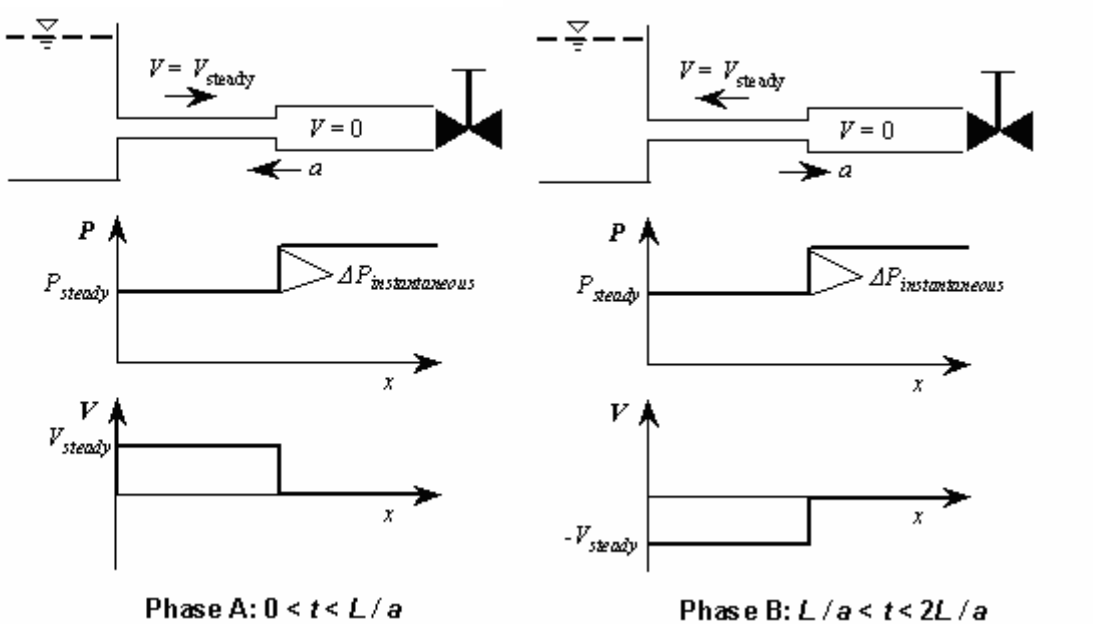

Phase A: $0 < t < L/a$ Phase B: $L/a < t < 2L/a$

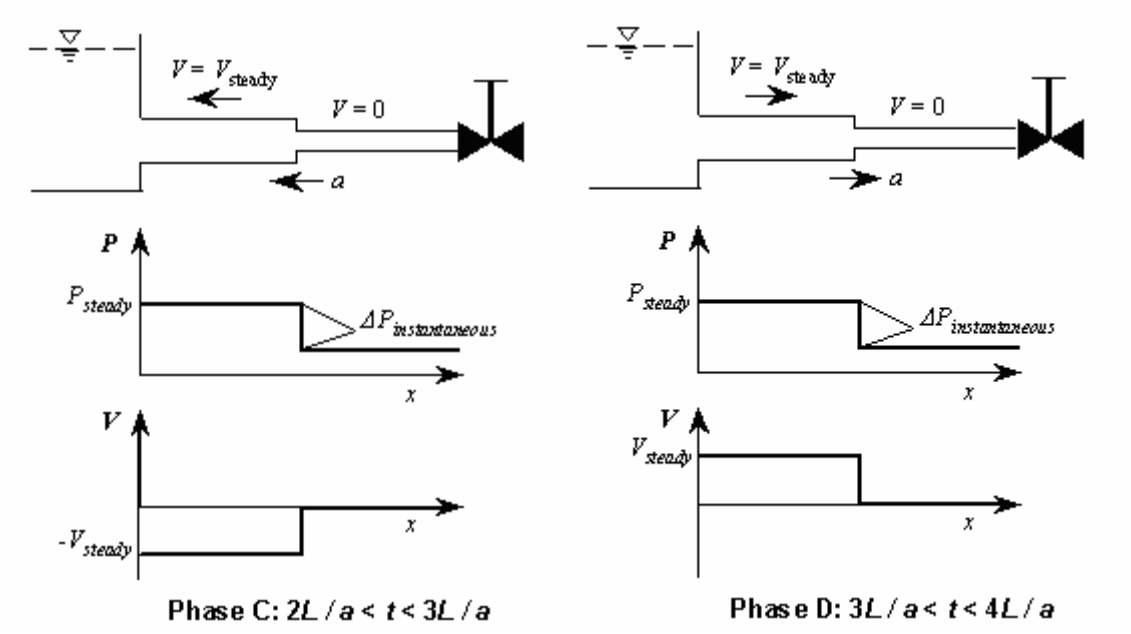

Fig 1.2: Pressure and velocity in a pipe after instantaneous valve closure.

Water hammer theory

The fundamental wave equations relating pressure and velocity in a conduit may be derived from consideration of Newton's law of motion and the conservation of mass respectively, and are:

$$\frac{\partial h}{\partial x}+\frac{1}{g}\frac{\partial v}{\partial t}+\frac{fv|v|}{2gd}=0$$

and

$$\frac{\partial h}{\partial t}+\frac{a^2}{g}\frac{\partial v}{\partial x}=0$$

Here friction is assumed to obey Darcy's equation with a constant friction factor f. The term "*a*" accounts for the elasticity of the fluid and pipe wall and is actually the celerity or speed of an elastic water hammer wave. This propagation speed is influenced by the piping material, wall thickness, diameter and structural support method. Thus wave speed is given by the following equation:

$$a = \frac{12}{\left[\frac{w}{g}\left(\frac{1}{K} + \frac{d}{Et}\right)\right]^{1/2}}$$

Where, a = wave velocity, ft/s

w = specific weight of fluid, lb/ft^3

K = Bulk modulus of compressibility of liquid, psi

E = Modulus of elasticity of pipe wall, psi

d = Inside diameter of pipe, in

t = Pipe wall thickness, in

g = Acceleration due to gravity, ft/s^2

Steady flow and water hammer analyses could provide information on the liquid behavior under operational conditions. Static pipe stress and structural dynamics analyses give insight to the corresponding behavior of the piping system; the structural dynamic analysis provides dynamics stress and reaction forces. Figure 1.3 shows the structural analysis element with its corresponding analyses.

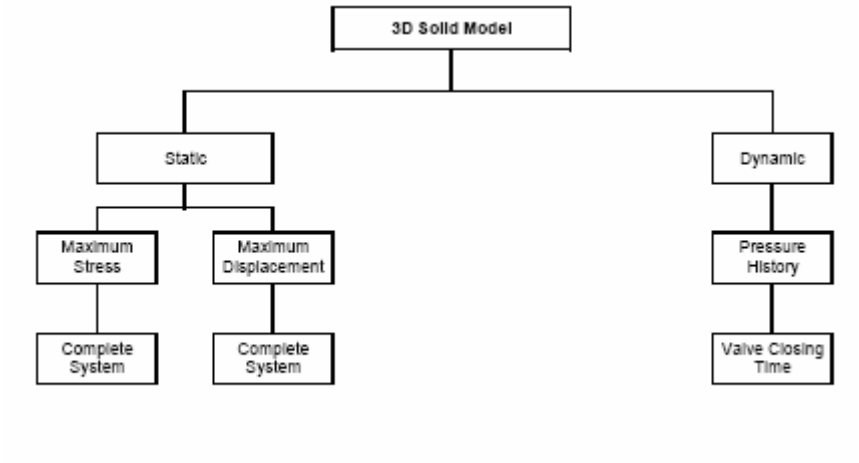

Fig: 1.3 Diagram of the structural study

1.2 Literature review

E.M.M. Fonseca, F. J. M. Q. de Melo and C. A. M. Oliveira [14] did the work on thermal and mechanical behavior of structural steel piping systems. They presented the thermal and mechanical analysis formulation for the structural steel piping systems. They did their work on piping systems of different end conditions subjected to elevated temperatures and found out the thermal displacements for the piping systems. Rudolph J. Scavuzzo, Jr. [16] did his work on effect of loading conditions on stress intensification factors of Mark's. Mark's method is based on determining the elastic plastic forces in a piping system by multiplying the elastic system stiffness by the actual deflection. Thus he calculated a fictitious force to determine piping stresses assuming the elastic beam bending equation, Mc/I, applies even in partially plastic pipes. Charles Becht IV and Yaofeng Chen [7] did their study on the effect of support span on the piping systems in their work. Pipe deflection due to self-weight quite often governs in the determination of the spacing between supports. They provided the solutions for the problem of establishing span limits for elevated temperature pipe. They gave the governing equations of deflection due to creep and produced the charts of determining the deflections for various spans of the supports for different end conditions. S. Chapuliot, D. Moulin and D. Plancq [9] presented a numerical and experimental study on the behavior of a branch pipe. They presented works on the branch pipe without soldering and without notching serving as reference for the analysis of the influence of the different parameters. They found out the stresses and strains near to the junctions for bending, pressure and the combination of bending and pressure. Raymond K. Yee and Marvin J. Kohn [8] did the study on creep relaxation behavior of the high energy piping. After prolonged operation of high energy piping systems at elevated temperatures, it is very difficult to evaluate the redistribution of stresses due to dead weight, pressure, external loading, and thermal loading. They evaluated the effect of a malfunctioning hanger on the distribution of stresses. Since hangers do not behave exactly as designed, it is important to determine the degree of increased stress and if the location of maximum stress can change due to a malfunctioning hanger. They used the results of elastic piping analysis of CAEPIPE for

estimating the relaxed and initial piping stresses. A.Khamlichi, L. Jezequel and F. Tephany [5] did the study on elastic-plastic water hammer analysis in the piping systems. They proposed a method of analysis based on the analogy existing between water hammer transients and longitudinal waves in a rod. They developed a finite difference scheme based on the method of characteristics to compute the plastic pressure waves in piping systems. The governing equations for wave propagation of pressure transients in a straight cylindrical pipe were obtained from the conservation of mass and momentum for one-dimensional analysis of this problem. The equations considered the pipe deformation effect under internal pressure. K. Kussmaul, E. Kobes, H. Diem, D. Schrammel and S. Brosi [4] conducted tests to investigate transient pipe loading initiated by a simulated double-ended guillotine break event, and subsequent closure of a feed water check valve (water hammer, blow-down). Numerical analyses by means of finite element programmes were performed in parallel to the experiments. The global behavior and loading of the nondamaged parts were determined by structural dynamics computations of the uncracked pipeline sections, with special pipe elements selected for the investigations. Benjamin R. Strong, Jr. and Ronald J. Baschiere [2] presented a method to determine steam/water hammer loads and blowdown thrust loads whereby the structural analyst can benefit by an accurate knowledge of the activity of the fluid within the piping system being studied. The method has its advantages in that a single approach may be utilized to simulate transients in water, steam and steam/water mixtures within general piping networks. For the development of the governing equation for the steam or water hammer loadings, they dealt with only the momentum equation and found the equations for the forces exerted by the fluid on the pipe. Yong W. Shin and William L Chen [1] described the method of characteristics as used to calculate fluid-hammer problems in complex piping networks. The formulation is based on the one-dimensional Navier-Stokes equation that contains the viscous term expressed as wall friction. A stepwise solution procedure being constructed from compatibility relations along characteristic and appropriate boundary conditions describing various types of pipe joints. Their paper discusses the method of characteristics as used in a general-purpose computer program for solving fluid-hammer problems in wide varieties of complex piping systems. The characteristic

method is formulated for the most general case of non-linear viscous flows with gravity effects included. Steady state flow conditions with minor pressure losses are used for the boundary conditions at sudden area changes, valves or orifices. They presented the characteristic formulation for the water hammer problem and the hydrodynamic equations for determining the pressure and velocity of the pressure wave. R. Gillessen & H. Lange [3] described the reduction of water hammer by active measures that mean the reduction of water hammer effects by influencing the fluid dynamic conditions of the system. Their work described a short outline of the production and analysis of water hammer, and also describes the fluid dynamic and design measures, which can be taken into account for this type of load. They considered the effect of valve closure time (fig-1.3), pipe lengths and reflection period of the pipe on the pressure also.

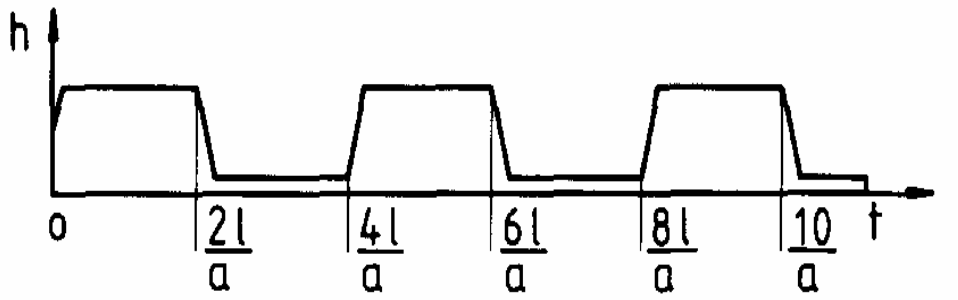

Fig 1.4: Rapid closing of the valve within the valve closing period

They also did the study for evaluating the effect of valve closure time on the flow rate. The following figure shows the variation of flow rate with valve closure time:

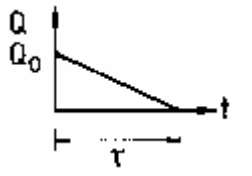

Fig 1.5: Flow rate variation with valve closure time.

For any time, t, the flow rate is given by the following equations:

$$Q(t) = Q_0(1 - \frac{t}{\tau}).....for(0 \le t \le \tau)$$

$$Q(t) = 0.....for(t > \tau)$$

Where Q_t is the flow rate at time t, Q_0 is the initial flow rate, τ is the valve closure time.

Jayaraj Kochupillai, N. Ganesan, Chandramouli Padmanabhan [13] presented a study to develop a simulation model for the fluid–structure interactions (FSI) that occur in pipeline systems mainly due to transient events such as rapid valve closing. They developed a new finite element formulation, based on flow velocity to deal with the valve closure transient excitation problems. M.A. Chaiko and K.W. Brinkman [10] presented a paper on the analysis of a piping system for water hammer with entrapped air with one-dimensional models. Calculations are carried out for a wide range of initial system pressure for getting the response of the piping system. They presented the governing equations for the water hammer phenomenon for the both liquid and gas region. E. Hadj Taieb and T. Lili [6] presented a mathematical formulation to describe the transient flow of homogeneous gas–liquid mixtures in deformable pipes. By application of the conservation of mass and momentum laws, a nonlinear hyperbolic system of two differential equations is obtained for the two principal dependent variables, which are the fluid pressure and velocity. A one-dimensional mathematical model that describes the transient behavior of gas–liquid mixture flow was presented. The model is based on the conventional water-hammer theory. S. A. Karamanos, E. Giakoumatos and A. M. Gresnigt [12] investigated the response of elbows under in-plane bending and pressure, through nonlinear finite element tools. They demonstrated the effects of pressure and the influence of straight pipe segments.

1.3 Objective

The following are the objectives of the project:

1. To do the static analysis of the piping system.
2. To do the thermal analysis of the piping system.
3. To carry out the transient flow analysis due to water hammer effect for closing of different valves.

Chapter 2

Static and Thermal Analysis

Static Analysis includes the measurement of

1. Stresses due to internal or external pressure.
2. Stresses due to weight of the fluid contained and weight of the piping system and attached components.
3. Thermal stresses.
4. Displacements due to combination of weight, pressure, and temperature.
5. Loads and moments on supports.
6. Element forces and moments due to weight, pressure and temperature.

The purpose of the static analysis of the piping system is to measure the above-mentioned forces, stresses, moments and displacements and to check the safety of the system against the failure due to these measured values.

2.1 Stress Categories

2.1.1 Primary Stresses:

These are developed by the imposed loading and are necessary to satisfy the equilibrium between external and internal forces and moments of the piping system. Primary stresses are not self-limiting i.e. these stresses continue to exist as long as the load persists and deformation does not stop.

2.1.2 Secondary Stresses:

These are developed by the constraint of displacements of a structure. These displacements can be caused either by thermal expansion or by outwardly imposed restraint and anchor point movements. Secondary stresses are self-limiting.

2.1.3 Peak Stresses:

Unlike loading condition of secondary stress, which causes distortion, peak stresses cause no significant distortion. Peak stresses are the highest stresses in the region under consideration and are responsible for causing fatigue failure

2.2 Classification of the loads

The following figure shows the classification of loads, which generally acts on a piping system: -

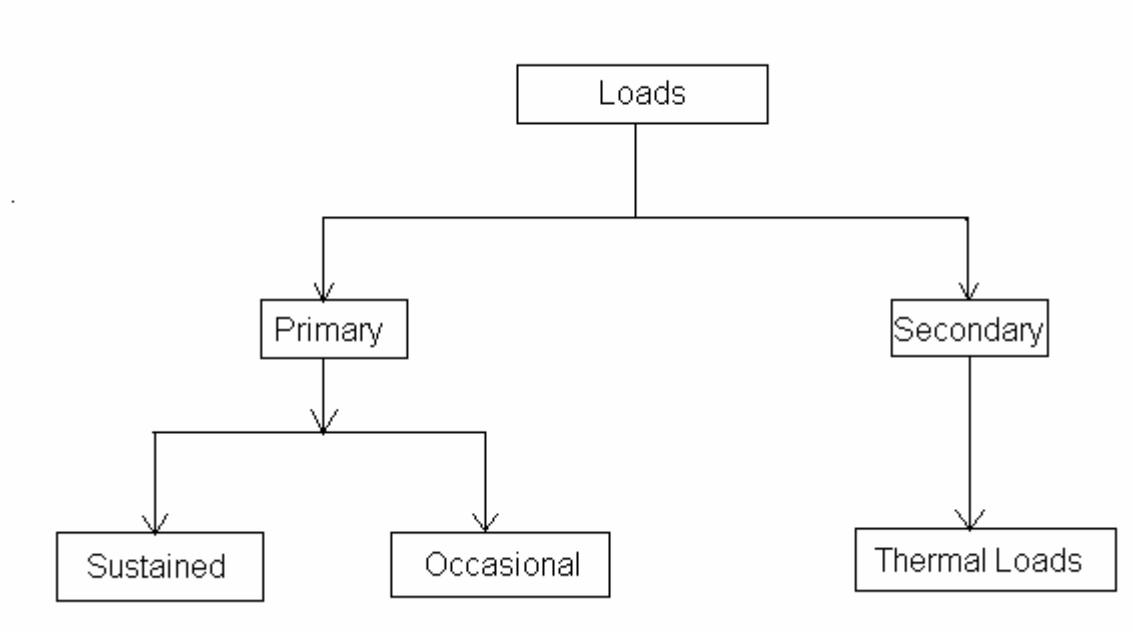

Figure 2.1: Classification of loads

2.2.1 Primary Loads

Primary loads can be divided into two categories based on the duration of the loading as follows-

- *Sustained Loads*: - These loads are expected to be present through out the plant operation such as internal fluid pressure, external pressure, gravitational forces acting on the pipe such as weight of pipe and fluid.
- *Occasional Loads*: - These loads are present at infrequent intervals during plant operation. e.g. earthquake, wind etc.

Primary loads are not self-limiting i.e. the stresses due to these loads continue to exist as long as the load persists. The system will continue to deform till rupture. Too large primary load can cause plastic deformation. Primary loads are not cyclic in nature.

Primary load causes the catastrophic failure. The design to prevent failure due to primary loads is based on one or more failure theories.

2.2.2 Secondary Loads

Secondary loads are caused by thermal displacement of piping. It results from restrained movements. A pipe may experience expansion or contraction once it is subjected to temperatures higher or lower respectively as compared to the temperature at which it was assembled. The secondary loads are often cyclic but not always. For example load due to tank settlement is not cyclic. A failure under such loads is often due to fatigue.

2.3 Stresses

2.3.1 Due to internal pressure

Internal fluid pressure produces both hoop (circumferential) stresses and longitudinal stresses as shown in the following figure.

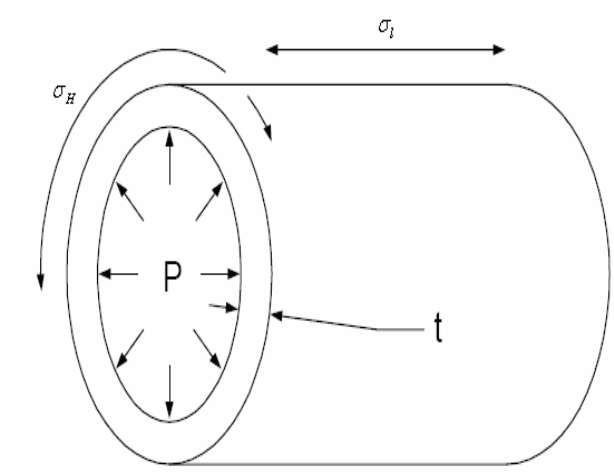

Figure 2.2: Stresses due to internal pressure

Where P is internal pressure, σ_H is hoop or circumferential stress, σ_l is longitudinal stress, t is pipe wall thickness.

2.3.1.1. Longitudinal Stress

Longitudinal stress σ_l due to internal pressure is given by

$$\sigma_l = F_L / A_m$$

$$A_m = \pi \times (d_o^2 - d_d^2)/4 - - - - - - - (a)$$
$$A_m = \pi \times (d_o + d_i) \times t/2 - - - - - - (b)$$
$$A_m = \pi \times d_0 \times t - - - - - - - - - - - - (c)$$

Where d_i is internal diameter of the pipe and F_L is the axial force exerted by the internal pressure. A_m is the cross sectional area of the pipe wall normal to the load direction. A_m can be given by the expressions as given above. Area can be calculated rigorously by equation (a), based on average diameter by equation (b) and based on outer diameter by equation (c).

If outer pipe diameter is used for calculating approximate metal cross section, the longitudinal stress due to internal fluid pressure can be found out as

$$\sigma_l = Pd_o/(4t)$$

2.3.1.2 Hoop stress

Due to internal fluid pressure, hoop stresses are induced in the pipe wall. From Membrane theory, σ_H may be approximated as

$$\sigma_H = Pd_o/2t$$

Or

$$\sigma_H = Pd_i/2t$$

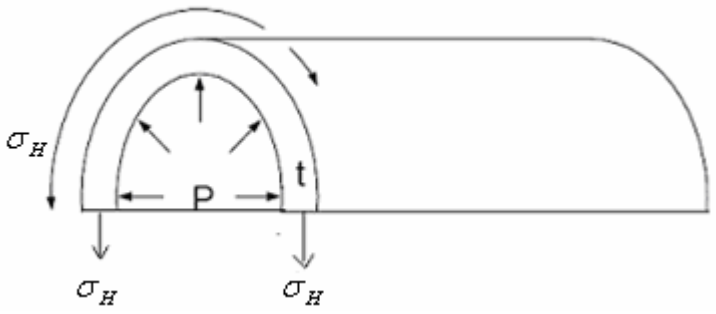

Fig 2.3: Hoop stresses due to internal pressure

2.3.2 Stresses due to axial force

Axial force can also cause the normal stress in the axial direction. The force may be tensile or compressive.

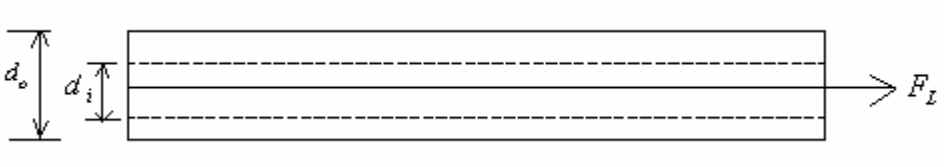

Fig 2.4: Axial Stresses

In the above figure the axial force F_L would lead to normal stress in the axial direction (σ_l). The load bearing cross section is the cross sectional area of the pipe wall normal to the load direction, A_m. The longitudinal stress then can be calculated as

$$\sigma_l = F_L / A_m$$

The load bearing cross section may be calculated rigorously or approximately as follows

$$A_m = \pi \times (d_o^2 - d_d^2)/4 \text{-------} (a)$$
$$A_m = \pi \times (d_o + d_i) \times t/2 \text{------} (b)$$
$$A_m = \pi \times d_0 \times t \text{-----------} (c)$$

Area can be calculated rigorously by equation (a), based on average diameter by equation (b) and based on outer diameter by equation (c).

2.3.3 Axial (longitudinal) stresses due to bending

Pipe bending is mainly due to two reasons: Uniform weight load and concentrated weight load. A pipe span supported at two ends would sag between these supports due to its own weight and the weight of the insulation (if any) when not in operation. It may sag due to its weight and the weight of the fluid it is carrying during operation. All these weights are distributed uniformly across the unsupported span and lead to maximum bending moment either at the centre of the span or at the end points of the span (support location) depending upon the type of the support used.

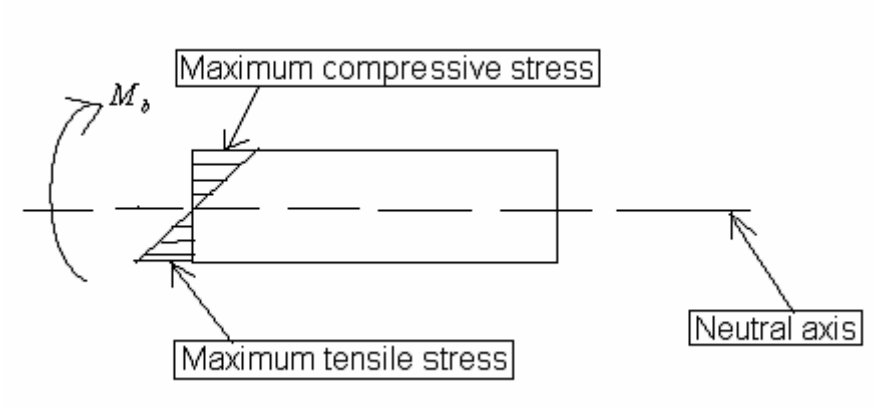

Fig 2.5: Axial stress due to bending

The axial stress changes from maximum tensile on one side of the pipe to maximum compressive on the other side. There is a neutral axis along which the bending moment does not induce any axial stresses. This is also the axis of the pipe.

The axial tensile stress for a bending moment of M_b at any location y as measured from the neutral axis is given as follows.

$$\sigma_l = M_b \times y / I$$

Where I is the moment of inertia of the pipe cross-section. For a circular cross-section pipe, I is given as

$$I = \pi \times (d_o^4 - d_i^4) / 64$$

The maximum tensile stress occurs where y is equal to the outer radius of the pipe and is given as follows:

$$\sigma_l = M_b \times r_o / I = M_b / Z$$

Where $Z = I / r_o$, is the section modulus of the pipe.

2.3.4 Shear stresses due to torsional load

Torsional load causes the shear stresses in pipe. The shear stress is maximum at the outer radius of the pipe. Shear stress at outer radius is given by the following expression:

$$\begin{aligned} \tau_{r=r_o} &= M_T r_o / R_T \\ &= M_T r_o / (2I) \\ &= M_T / (2Z) \end{aligned}$$

Where $\tau_{r=r_o}$ is the shear stress due to torsion at outer radius, M_T is the torsional moment, R_T is the torsional resistance, Z is the section modulus, I is the moment of inertia.

Thus following stresses can be considered under static stress analysis:

1. Longitudinal stresses: Summation of the longitudinal stresses due to internal pressure, axial force and bending moment as given below:

$$\sigma_L = F_L / A_m + Pd_o / 4t + M_b / Z$$

2. Hoop stresses:

$$\sigma_H = Pd_o / 2t$$

3. Shear stresses:

$$\tau_{r=r_o} = M_T / 2Z$$

2.4 Theories of Failure

2.4.1 Maximum Stress Theory

This is also called Rankine theory. According to this theory, failure occurs when the maximum principal stress in a system is greater than the maximum tensile principal stress at yield in a specimen subjected to uniaxial tension test.

In uniaxial test hoop stress and radial stress and shear stresses are absent. Thus longitudinal stress is the normal principal stress. Thus the following equations holds

$$\sigma_L = \sigma_Y, \sigma_H = 0, \sigma_R = 0$$
$$\sigma_1 = \sigma_Y, \sigma_2 = 0, \sigma_3 = 0$$

The maximum tensile principal stress at yield is thus equal to the yield stress. The Rankine theory thus just says that failure occurs when the maximum principal stress in a system (σ_1) is more than the yield stress of the material (σ_Y). This theory forms the basis for the piping system governed by ASME B31.3.

2.4.2 Maximum Shear Stress Theory

This theory states that failure of a piping component occurs when the maximum shear stress exceeds the shear stress at the yield point in a tensile test. In the tensile test, at yield, $\sigma_1 = \sigma_Y, \sigma_2 = \sigma_3 = 0$. So yielding in the components occurs when

$$\text{Maximum Shear stress} = \tau_{\max} = (\sigma_1 - \sigma_2)/2 = \sigma_Y / 2$$

2.5 Allowable stresses

Allowable stresses specified by the code can be classified into two categories-

2.5.1 Time independent stresses

Time independent allowable stress is based on either yield stress or the ultimate tensile strength measured in a simple tensile test. The ultimate tensile strength is the highest stress, which the specimen can sustain without failure. As per ASME B 31.3 the basic allowable material stress at the hot or operating/design condition is defined as minimum of

i) 1/3 of the ultimate tensile strength of the material at operating temperature.

ii) 1/3 of the ultimate tensile strength of the material at room temperature.

i) 2/3 of the yield strength of the material at the operating temperature.

ii) 2/3 of the yield strength of the material at the room temperature.

2.5.2 Time dependent stresses

These stresses are defined as the creep rupture strength at high temperature. If the temperature is more than 1/3 of the melting point, the metal exhibits the creep.

The smaller value of the time dependent and time independent stress is taken as the allowable stress value.

2.6 Allowable expansion stress range

Thermal stresses or the expansion stresses are cyclic in nature. The hot stresses decrease with time but the sum of the hot and cold stresses remains same. This sum is called as the expansion stress range.

Maximum stress range to which the piping system can be subjected to is given by the following equation

$$\sigma_{\max} = 1.6\sigma_c + 1.6\sigma_h$$

The American design codes ASME B 31.1 and B31.3 limit the stress range to 78% of the yield stress. Thus the above expression can be reduced to following form

$$\sigma_{allowable} = 1.6 \times 0.78 \times (\sigma_c + \sigma_h)$$
$$\sigma_{allowable} = 1.25(\sigma_c + \sigma_h)$$

In this expression, out of $1.25\sigma_h$, one σ_h is used for the longitudinal stresses developed due to loading such as pressure, weight and other sustained loading. Thus the allowable stress range for the flexibility will be as follows

$$\sigma_{allowable} = 1.25(\sigma_c + \sigma_h) - \sigma_h$$

or

$$\sigma_{allowable} = 1.25\sigma_c + 0.25\sigma_h$$

For considering the excessive cyclic conditions the above expression should be multiplied by a stress range reduction factor. Thus the Allowable Stress Range will be given by the following expression

$$\sigma_{allowable} = f(1.25\sigma_c + 0.25\sigma_h)$$

Where,

$\sigma_{allowable}$ = Allowable expansion stress range

σ_c = Basic allowable stress at minimum metal temperature during the displacement cycle under analysis

σ_h = Basic allowable stress at maximum metal temperature during the displacement cycle under analysis

f = Stress range reduction factor for displacement cycle conditions for the total number of cycles over the expected life. Following table gives the stress range reduction factor for various numbers of cycles: -

Cycles N	**Factor f**
7000 or less	1.0
Over 7000 to 14000	0.9
Over 14000 to 22000	0.8
Over 220000 to 45000	0.7
Over 45000 to 100000	0.6
Over 100000 to 200000	0.5
Over 200000 to 700000	0.4
Over 700000 to 2000000	0.3

Table 2.1: Stress range reduction factors

When the basic allowable stress at maximum expected metal temperature σ_h, is greater than the sum of the longitudinal stresses due to pressure, weight and other sustained

loading σ_L the difference between them is added to the term $0.25\sigma_h$ in the equation for for $\sigma_{allowable}$. Thus the allowable stress range in that case will be

$$\sigma_{allowable} = f[1.25(\sigma_c + \sigma_h) - \sigma_L]$$

2.7 Flexibility factor and Stress Intensification Factor

Bend: - The ratio of the flexibility of a bend to that of a straight pipe having the same length and cross section is known as its flexibility factor usually denoted by "k".

The circumferential stresses due to bending moment M in a bend or elbow can be many times the value of longitudinal stresses (My/I) obtained by bending theory of structural members. The factor by which the circumferential stresses exceed the longitudinal stresses in the bend is called the "Stress Intensification Factor or S.I.F.".

Appendix D of ASME B31.3 gives the expressions to be used for calculating the flexibility factor and stress intensification factor. The parameter used for the calculation of these factors is called the flexibility characteristic denoted by "h".

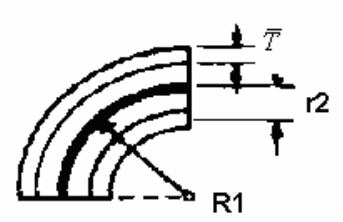

Fig 2.6: Bend flexibility

For bend,

Flexibility characteristic, $h = \frac{\bar{T}R_1}{r_2^2}$ …….. (1)

The flexibility factor, $k = \frac{1.65}{h}$ …….. (2)

In-plane S.I.F., $I_i = \frac{0.9}{h^{2/3}}$ …… (3)

Out-plane S.I.F., $I_o = \frac{0.75}{h^{2/3}}$ …….. (4)

Where,

R_1 = Bend radius

$\bar{T}$ = Nominal wall thickness of fitting

r_2 = Mean radius of pipe

2.7.1 Calculation for SIFs of bend

R_1 = Bend radius = 1.5”

$\bar{T}$ = Nominal wall thickness of fitting = 0.133”

r_2 = Mean radius of pipe = 0.591”

Thus Flexibility characteristic, from equation (1)

$$h = \frac{\bar{T}R_1}{r_2^2}$$

$$h = 0.571$$

The flexibility factor, from equation (2)

$$k = \frac{1.65}{h}$$

$$k = 2.89$$

In-plane S.I.F., from equation (3)

$$I_i = \frac{0.9}{h^{2/3}}$$

$$I_i = 1.30$$

Out-plane S.I.F., from equation (4)

$$I_o = \frac{0.75}{h^{2/3}}$$

$$I_o = 1.09$$

The following table shows the values of in plane and out-planes SIF values calculated by CAEPIPE and shows the comparison of these values obtained by the calculations.

	S.I.F.	
	In-plane, I_i	Out-plane, I_o
By, calculation	1.30	1.09
By, CAEPIPE	1.30	1.09

Table 2.2: SIFs for bend

2.8 Requirements of ASME B 31.3

This code governs all piping within the property limits of facilities engaged in the processing or handling of chemical, petroleum or related products. Examples are a chemical plant, petroleum refinery, loading terminal, natural gas processing plant, bulk plant, compounding plant and tank farm**.**

The loadings required to be considered are pressure, weight (live and dead loads), impact, wind, earthquake-induced horizontal forces, vibration discharge reactions, thermal expansion and contraction, temperature gradients, anchor movements.

The governing equations are as follows: -

2.8.1 Stresses due to sustained loads.

$$\sigma_L \leq \sigma_h$$

Where σ_L can be given by the following expression

$$\sigma_L = F_L / A_m + Pd_o / 4t + [(I_i M_i)^2 + (I_o M_o)^2]^{0.5} / Z$$

σ_L = Sum of longitudinal stresses due to pressure, weight and other sustained loading, psi

F_L = Axial force due to sustained loading, lbs

A_m = Metal cross section area, in^2

M_i = In plane bending moment due to sustained loading, in-lb

M_o = Out plane bending moment due to sustained loading, in-lb

I_i, I_o = In plane and out plane stress intensification factors

σ_h = Basic allowable stress at the operating temperature

2.8.2 Stresses due to occasional loads.

The sum of the longitudinal loads due to pressure, weight and other sustained loads and of stresses produced by occasional loads such as earthquake or wind shall not exceed $1.33\sigma_h$.

2.8.3 Stress range due to expansion loads.

The displacement stress range σ_E shall not exceed $\sigma_{allowable}$:

$$\sigma_E \leq \sigma_{allowable}$$

Where,

$$\sigma_E = (\sigma_b^2 + 4\sigma_t^2)^{1/2} / Z$$

The resultant bending stress σ_b can be given by the following equation

$$\sigma_b = [(I_i M_i)^2 + (I_o M_o)^2]^{0.5} / Z$$

σ_t is the torsional stress, which is given by the following expression

$$\sigma_t = M_t / 2Z$$

Mi = in-plane bending moment, in.lb

Mo = out-plane bending moment, in.lb

Ii = in- plane stress intensification factor obtained from appendix of B31.3

Io = out- plane stress intensification factor obtained from appendix of B31.3

σ_t = Torsional stress, psi

Z = Section modulus of pipe, in^3

2.9 Model

The three dimensional model has been created in piping modeling and analysis software, CAEPIPE. For the analysis purpose this software provides a list of various codes. For our case ASME B 31.3 has been selected for the analysis.

The model has following elements:

1. Three ball valves.
2. One bend of long radius.
3. Twelve pipe segments.

The model also has following Data Types:

1. One flange.
2. Two anchors.
3. Four restraints.

The material of the pipe is ASTM 312 TP 304L (stainless steel). The pipeline is having an outer diameter of 1.315", inside diameter of 1.049" and a thickness of 0.133" with schedule number of 40. The fluid inside the pipe is methanol at a temperature of 185 F and a pressure of 165 psi.

2.9.1 Assumptions

The connected equipments at the node 60 and 150 have not been included in the analysis. The connection of theses equipment with the piping system has been modeled as anchors. All the six degrees of freedom of the anchors were held fixed. The weight of the valves and flange has been included in the analysis.

The following table shows the pipe properties:

NPS	O.D.	I.D.	Thickness	Material
1”	1.315”	1.049”	0.133”	ASTM A312TP304L

Table 2.3: Pipe properties

Chemical Composition of ASTM A312TP304L

Manganese	Silicon	Sulpher	Phosphorus	Chromium	Nickel
2%	1%	0.030%	0.045%	18-20%	8-12%

Table 2.4: Chemical composition of ASTM A312TP304L

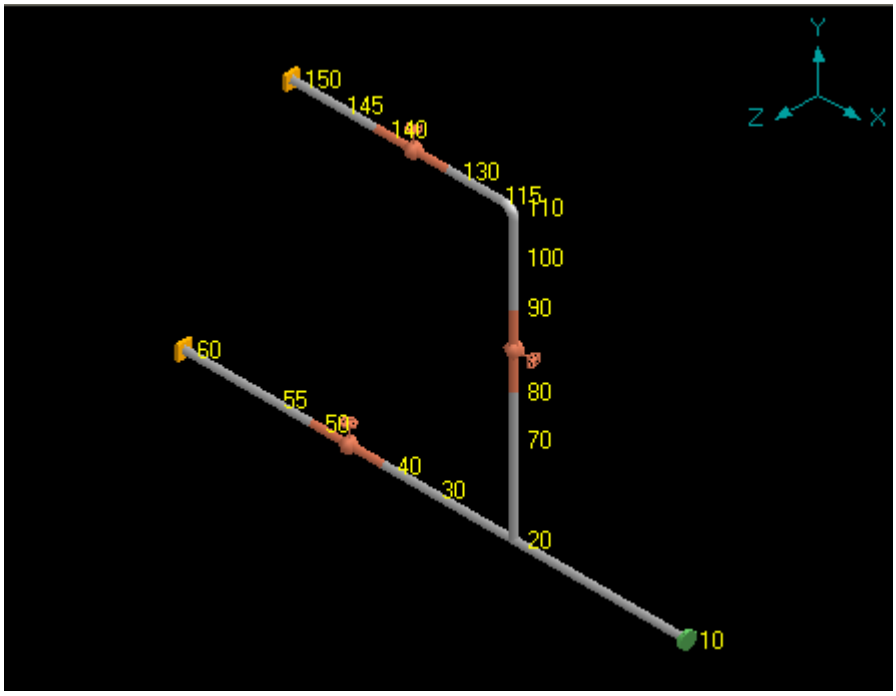

Fig 2.7: 3-Dimensional model of the piping system

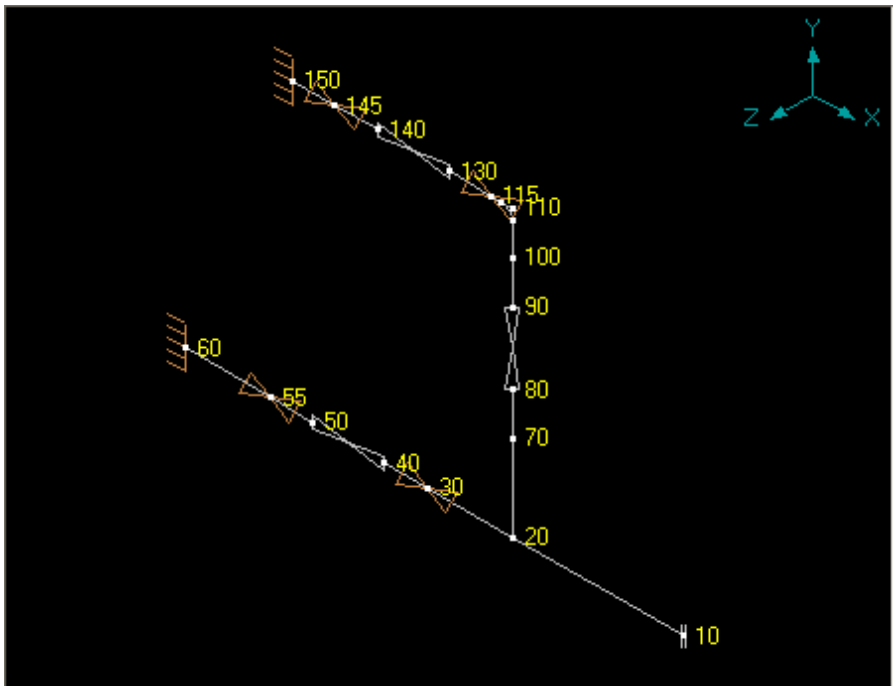

Fig 2.8: Wire mesh model of the piping system

2.10 Load Cases

In our case, the piping system has only one pressure and one temperature; therefore load cases for the purpose of analysis should be as follows:

1. L1 = W+T1+P1 (OPE)
2. L2 = W+P1 (SUS)
3. L3 = T1 (EXP)

While doing analysis of the piping system, besides checking nodal loads or restraint loads, code stresses should also be checked. If percentage of code stress check is higher than 100% i.e. the ratio of maximum stress/allowable stress is more than 1, then the system will fail, whatever may be the nodal or restraint loads. For stress check, load cases L2 and L3 should be selected and for displacements and load check, load cases L1 and L2 should be selected.

2.11 Results

The following figure shows the stress ratios for sustained load case (L2 = W+P1) in the nodes in the piping system.

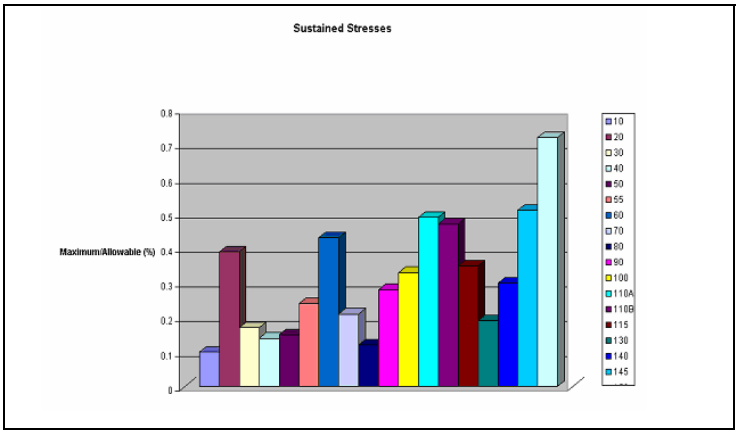

Fig 2.9: Sustained stress ratios for nodes

From the figure it is clear that the sustained stresses in the piping system do not create any problem, as the highest value of maximum stress/allowable ratio is 0.72 for the node number 150. Thus all the stress ratios are less than 1.The values of the sustained stresses in these nodes can be obtained from the following table, as obtained from the CAEPIPE software.

#	Sustained			
	Node	SL (psi)	SH (psi)	SL / SH
1	150	12011	16700	0.72
2	145	8438	16700	0.51
3	110A	8218	16700	0.49
4	110B	7892	16700	0.47
5	60	7236	16700	0.43
6	20	6554	16700	0.39
7	115	5840	16700	0.35
8	100	5557	16700	0.33
9	140	5011	16700	0.30
10	90	4021	16700	0.24
11	55	3971	16700	0.24
12	70	3513	16700	0.21
13	130	3236	16700	0.19
14	30	2847	16700	0.17
15	50	2556	16700	0.15
16	40	2336	16700	0.14
17	80	1993	16700	0.12
18	10	1644	16700	0.10

Table 2.5: Sustained Stress Values

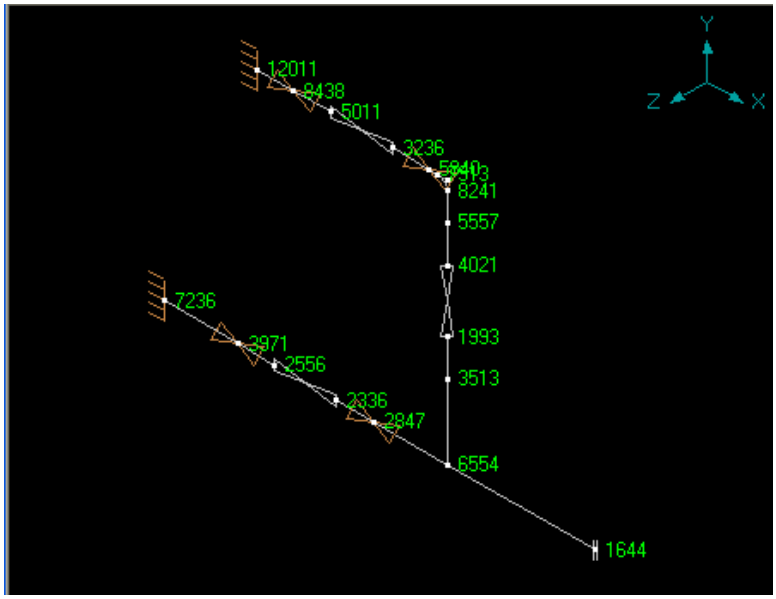

Fig 2.10: Sustained Stress Distribution in the piping system in wire mesh model

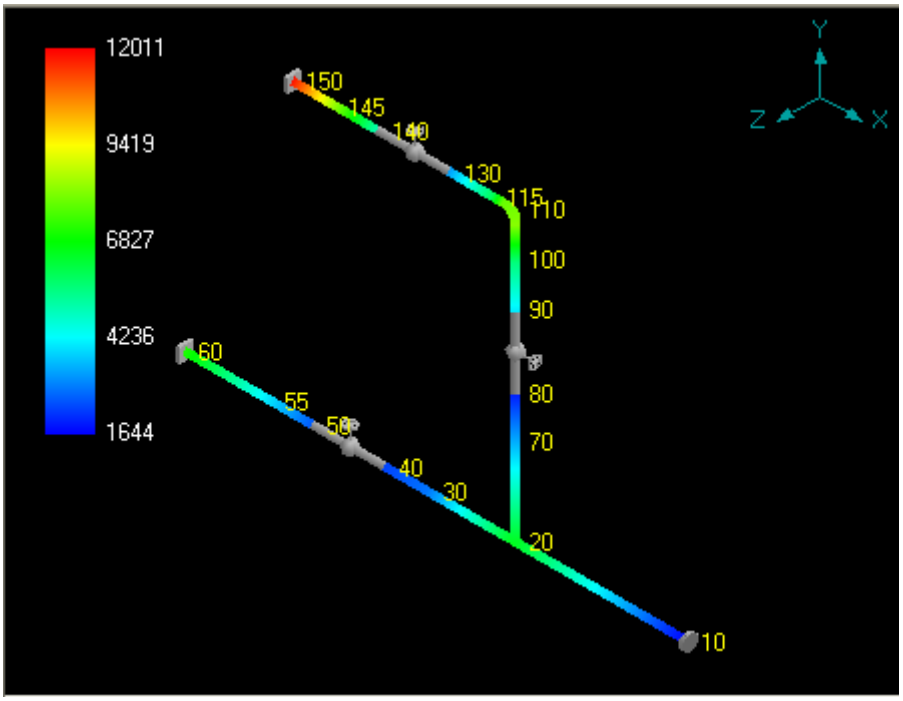

Fig 2.11: Sustained Stress Distribution in the piping system in solid model

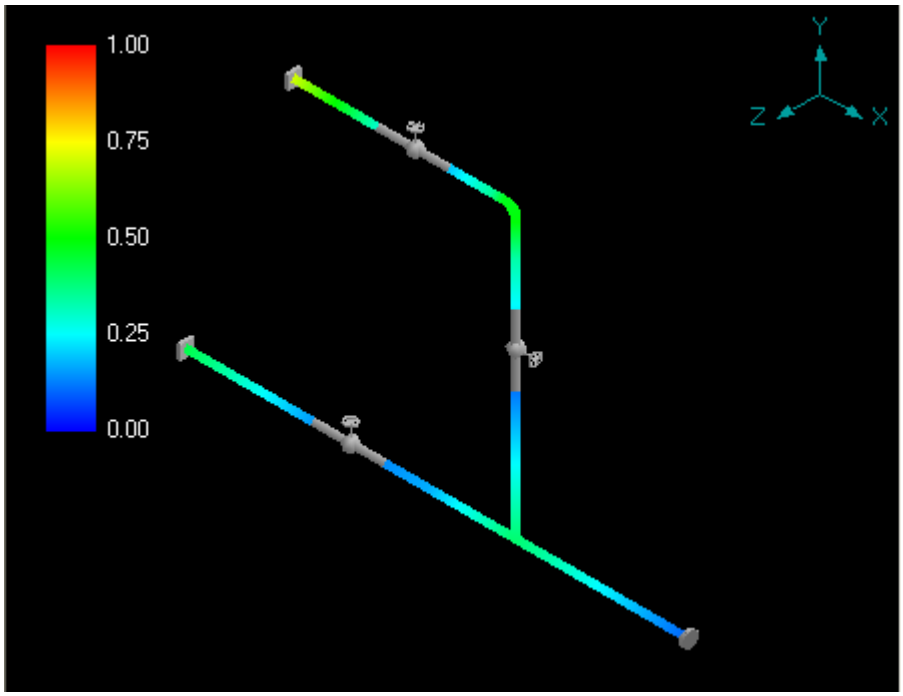

Fig 2.12: Stress ratios for sustained load case

2.11.1 Supports and Restraints report

A. Forces and Moments on Anchor at node 60

The figure shows the values of forces and moments on anchor at node 60 for sustained, operating and expansion load cases. The sustained stress ratio value at node 60 is found to be 0.43 (table 2.5). For expansion load case the value of stress ratio was 0.91 (table 2.22). Thus the results show that the values obtained for all these load cases are within the safe limits.

Load combination	FX (lb)	FY (lb)	FZ (lb)	MX (ft-lb)	MY (ft-lb)	MZ (ft-lb)
Sustained	0	-12	0	0	0	-19
Operating	-14970	-18	0	0	0	-33
Maximum	0	-12	0	0	0	-19
Minimum	-14970	-18	0	0	0	-33

Table 2.6: Support load summary for anchor at node 60

FX (lb)	FY (lb)	FZ (lb)	MX (ft-lb)	MY (ft-lb)	MZ (ft-lb)
-14970	-6	0	0	0	-13

Table 2.7: Support load summary for anchor at node 60: Expansion load

From the above tables and the figures it is clear that the maximum negative force in X-direction is obtained in operating load case. For operating load case the numerical values of FY and MZ is very less as compared to the value of FX.

B. Forces and Moments on Anchor at node 150

The following figures gives the values of forces and moments obtained for the sustained and operating load cases for anchor at node 150. At this node only the expansion stress was just more than the allowable limits. The stress ratio for expansion

load case was 1.06 (table 2.22). The stress ratio for sustained load case was 0.72 (table 2.5). Thus the anchor is just safe.

Load Combination	FX (lb)	FY (lb)	FZ (lb)	MX (ft-lb)	MY (ft-lb)	MZ (ft-lb)
Sustained	0	-25	0	0	0	-36
Operating	-14970	-19	0	0	0	-23
Maximum	0	-19	0	0	0	-23
Minimum	-14970	-25	0	0	0	-36

Table 2.8: Support load summary for anchor at node 150

FX (lb)	FY (lb)	FZ (lb)	MX (ft-lb)	MY (ft-lb)	MZ (ft-lb)
-14970	6	0	0	0	13

Table 2.9: Support load summary for anchor at node 150- Expansion load

From the above tables and figures it is clear that the results for expansion load (Temperature) case can be obtained by subtracting the results of sustained load case (weight and pressure loads combination) from the results of operating load cases (weight, pressure and temperature loads combination). Also the results show that these forces and moments are not dangerous for the anchor and thus the piping system.

C. Support load summary for restraint at node 30

Load combination	FX (lb)	FY (lb)	FZ (lb)
Sustained	-11		
Operating	22359		
Maximum	22359		
Minimum	-11		

Table 2.10: Load summary of restraint at node 30

D. Support load summary for restraint at node 55

Load combination	FX (lb)	FY (lb)	FZ (lb)
Sustained	0		
Operating	-7402		
Maximum	0		
Minimum	-7402		

Table 2.11: Load summary of restraint at node 55

E. Support load summary for restraint at node 115

Load combination	FX (lb)	FY (lb)	FZ (lb)
Sustained	11		
Operating	22384		
Maximum	22384		
Minimum	11		

Table 2.12: Load summary of restraint at node 115

F. Support load summary for restraint at node 145

Load combination	FX (lb)	FY (lb)	FZ (lb)
Sustained	0		
Operating	-7402		
Maximum	0		
Minimum	-7402		

Table 2.13: Load summary of restraint at node 145

Since all the restraints have been put in the X-direction only, the forces for sustained and operating load conditions are in the X-direction only. The forces in Y and Z direction are zero for all the restraints. CAEPIPE shows that these results are within the limits except due to expansion load case where the stress ratios were 1.39 for node 145, 1.26 for node 115, 1.22 for node 55 and 1.17 for node 30 (table 2.22).

2.11.2 Displacements

Different load case causes the displacements of the piping system. These displacements are the results of the displacements of the nodes of the piping system. The following table shows the displacements of the nodes for sustained and operating load conditions:

Direction	Type	Value	Node
X	Minimum	-0.002	100
(inch)	Maximum	0.002	70
Y	Minimum	-0.056	10
(inch)	Maximum	0.000	60
Z	Minimum	0.000	10
(inch)	Maximum	0.000	10
XX	Minimum	0.000	10
(deg)	Maximum	0.000	10
YY	Minimum	0.000	10
(deg)	Maximum	0.000	10
ZZ	Minimum	-0.081	130
(deg)	Maximum	0.0135	80

Table 2.14: Minimum and Maximum Displacements: Sustained Load Case (L2)

Above table shows the maximum and minimum displacements in each direction. The maximum displacement in X direction was found at node 70 and minimum displacement in X direction was at node 100. In Y direction maximum displacement was at node 10 and maximum displacement was at node 60. In Z direction maximum and minimum displacements were found zero at node 10. Maximum and minimum rotational displacements about X and Y axes were found zero, all at node 10. In Z direction the maximum rotational displacement was at node 80 and minimum was at node 130.

CAEPIPE does not show the failure of the piping system due to the excessive displacements of any of the nodes.

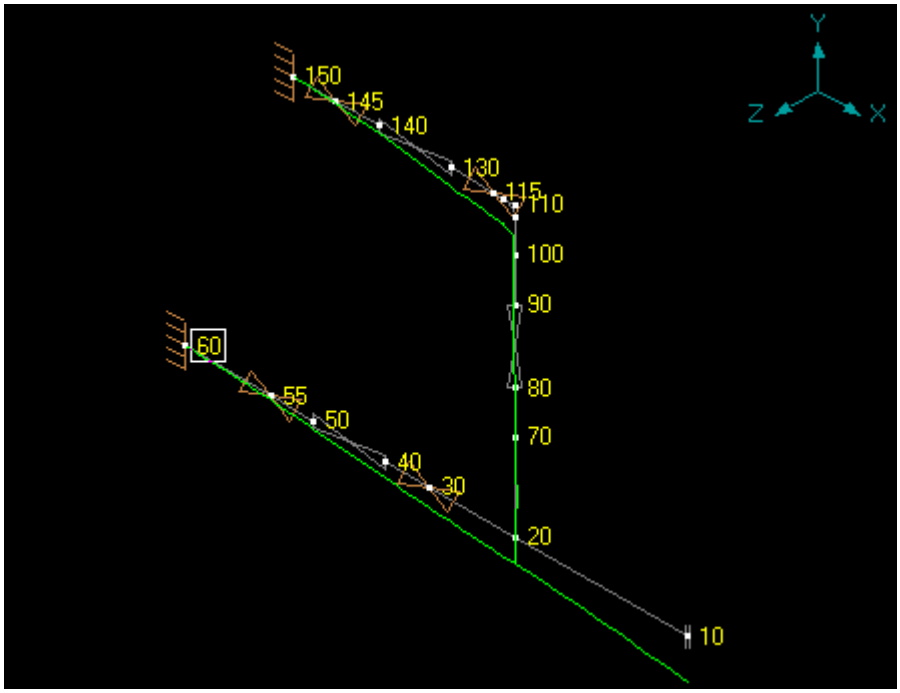

Fig 2.13: Deflected shape- Sustained Load Case (L2)

Direction	Type	Value	Node
X	Minimum	-0.003	50
(inch)	Maximum	0.039	10
Y	Minimum	-0.092	10
(inch)	Maximum	0.000	60
Z	Minimum	0.000	10
(inch)	Maximum	0.000	10
XX	Minimum	0.000	10
(deg)	Maximum	0.000	10
YY	Minimum	0.000	10
(deg)	Maximum	0.000	10
ZZ	Minimum	-0.0994	40
(deg)	Maximum	0.0333	90

Table 2.15: Minimum and Maximum Displacements-Operating loads case (L1)

Above table shows maximum and minimum displacements and rotations in X, Yand Z direction. For the operating load case also it is found out that the system is safe.

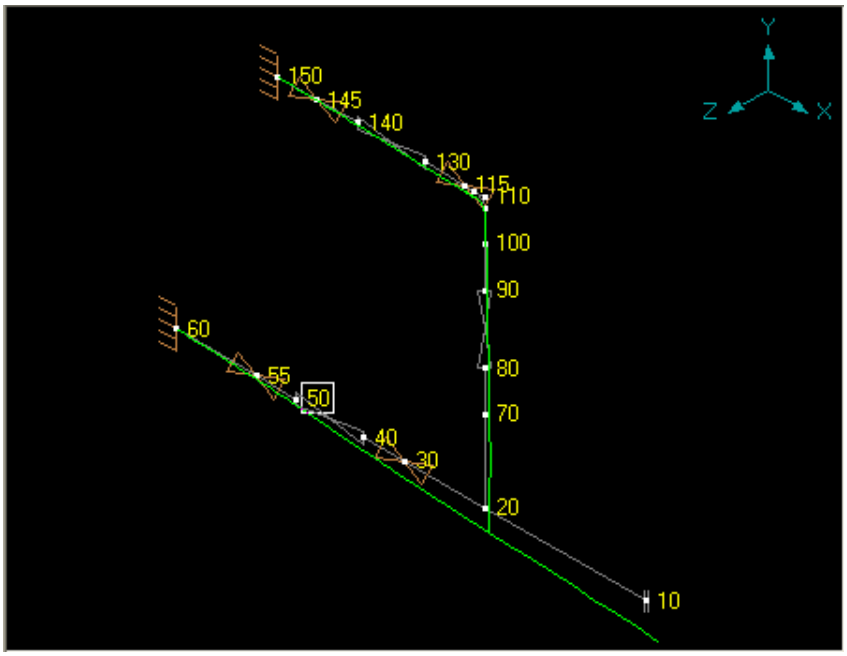

Fig 2.14: Deflected shape - operating load case (L1)

2.11.3 Pipe and element forces

A. Sustained Load Case (L2)

i) Pipe forces

The table below shows the forces in the pipe due to sustained loading. The results obtained by CAEPIPE here are acceptable as all the nodes have the loads within safe limits. These results give the values of the forces in the straight pipe sections only as it is clear from the following table.

#	Node	FX (lb)	FY (lb)	FZ (lb)	MX (ft-lb)	MY (ft-lb)	MZ (ft-lb)
1	10 20	0 0	-3 7	0 0	0 0	0 0	0 11
2	20 30	-11 11	-1 3	0 0	0 0	0 0	6 -4
3	30 40	0 0	-3 4	0 0	0 0	0 0	4 -2
4	50 55	0 0	-9 10	0 0	0 0	0 0	-3 8
5	55 60	0 0	-10 12	0 0	0 0	0 0	-8 19
6	20 70	11 -11	-6 8	0 0	0 0	0 0	-17 6
7	70 80	11 -11	-8 9	0 0	0 0	0 0	-6 1
8	90 100	11 -11	-15 16	0 0	0 0	0 0	8 -13
9	100 110A	11 -11	-16 16	0 0	0 0	0 0	13 -17
10	110A 110B	11 -11	-16 17	0 0	0 0	0 0	17 -16
11	110B 115	11 -11	-17 17	0 0	0 0	0 0	16 -14
12	115 130	0 0	-17 18	0 0	0 0	0 0	14 -6
13	140 145	0 0	-23 24	0 0	0 0	0 0	-12 24
14	145 150	0 0	-24 25	0 0	0 0	0 0	-24 36

Table 2.16: Pipe forces-Sustained load

ii) Element forces

CAEPIPE gives the values for the forces and moments in X, Y, Z directions for the elements in the entire piping system also as shown in the table below. From the results for these forces for sustained load case, all the elements were found out safe for against failure. Thus the piping system is safe against these loading conditions.

Node	***FX (lb)***	***FY (lb)***	***FZ (lb)***	***MX (ft-lb)***	***MY (ft-lb)***	***MZ (ft-lb)***
10 20	0 0	-3 7	0 0	0 0	0 0	0 11

20 30	-11 11	-1 3	0 0	0 0	0 0	6 -4
30 40	0 0	-3 4	0 0	0 0	0 0	4 -2
40 50	0 0	-4 9	0 0	0 0	0 0	2 3
50 55	0 0	-9 10	0 0	0 0	0 0	-3 8
55 60	0 0	-10 12	0 0	0 0	0 0	-8 19
20 70	11 -11	-6 8	0 0	0 0	0 0	-17 6
70 80	11 -11	-8 9	0 0	0 0	0 0	-6 1
80 90	11 -11	-9 15	0 0	0 0	0 0	-1 -8
90 100	11 -11	-15 16	0 0	0 0	0 0	8 -13
100 110A	11 -11	-16 16	0 0	0 0	0 0	13 -17
110A 110B	11 -11	-16 17	0 0	0 0	0 0	17 -16
110B 115	11 -11	-17 17	0 0	0 0	0 0	16 -14
115 130	0 0	-17 18	0 0	0 0	0 0	14 -6
130 140	0 0	-18 23	0 0	0 0	0 0	6 12
140 145	0 0	-23 24	0 0	0 0	0 0	-12 24

145 150	0 0	-24 25	0 0	0 0	0 0	-24 36

Table 2.17: Element forces-Sustained load

B. Operating Load Case (L1)

i) Pipe forces

The table below shows the forces in the pipe due to operating loading. The results obtained by CAEPIPE here are acceptable as all the nodes have the loads within safe limits. These results give the values of the forces in the straight pipe sections only as it is clear from the following table

#	Node	FX (lb)	FY (lb)	FZ (lb)	MX (ft-lb)	MY (ft-lb)	MZ (ft-lb)
1	10 20	0 0	-3 7	0 0	0 0	0 0	0 11
2	20 30	-13 13	-7 9	0 0	0 0	0 0	16 -8
3	30 40	-22372 22372	-9 10	0 0	0 0	0 0	8 -3
4	50 55	-22372 22372	-15 16	0 0	0 0	0 0	-8 15
5	55 60	-14970 14970	-16 18	0 0	0 0	0 0	-15 33
6	20 70	13 -13	0 2	0 0	0 0	0 0	-26 14
7	70 80	13 -13	-2 3	0 0	0 0	0 0	-14 7
8	90 100	13 -13	-9 10	0 0	0 0	0 0	3 -10
9	100 110A	13 -13	-10 10	0 0	0 0	0 0	10 -15
10	110A 110B	13 -13	-10 11	0 0	0 0	0 0	15 -15
11	110B 115	13 -13	-11 11	0 0	0 0	0 0	15 -13
12	115 130	-22372 22372	-11 12	0 0	0 0	0 0	13 -8
13	140 145	-22372 22372	-17 18	0 0	0 0	0 0	-5 14
14	145 150	-14970 14970	-18 19	0 0	0 0	0 0	-14 23

Table 2.18: Pipe forces - operating load

ii) Element forces

CAEPIPE gives the values for the forces and moments in X, Y, Z directions for the elements in the entire piping system also as shown in the table below. From the results for these forces for operating load case, all the elements were found out safe against failure. Thus the piping system is safe against these loading conditions.

Node	***FX (lb)***	***FY (lb)***	***FZ (lb)***	***MX (ft-lb)***	***MY (ft-lb)***	***MZ (ft-lb)***

10 20	0 0	-3 7	0 0	0 0	0 0	0 11
20 30	-13 13	-7 9	0 0	0 0	0 0	16 -8
30 40	-22372 22372	-9 10	0 0	0 0	0 0	8 -3
40 50	-22372 22372	-10 15	0 0	0 0	0 0	3 8
50 55	-22372 22372	-15 16	0 0	0 0	0 0	-8 15
55 60	-14970 14970	-16 18	0 0	0 0	0 0	-15 33
20 70	13 -13	0 2	0 0	0 0	0 0	-26 14
70 80	13 -13	-2 3	0 0	0 0	0 0	-14 7
80 90	13 -13	-3 9	0 0	0 0	0 0	-7 -3
90 100	13 -13	-9 10	0 0	0 0	0 0	3 -10
100 110A	13 -13	-10 10	0 0	0 0	0 0	10 -15
110A 110B	13 -13	-10 11	0 0	0 0	0 0	15 -15
110B 115	13 -13	-11 11	0 0	0 0	0 0	15 -13
115 130	-22372 22372	-11 12	0 0	0 0	0 0	13 -8
130 140	-22372 22372	-12 17	0 0	0 0	0 0	8 5

140 145	-22372 22372	-17 18	0 0	0 0	0 0	-5 14
145 150	-14970 14970	-18 19	0 0	0 0	0 0	-14 23

Table 2.19: Element forces - operating load

2.11.4 Forces on valve nodes

A. Operating load case (L1)

Forces on valve nodes are obtained by applying the different load cases on to the model. Valves have been assumed to connect to two nodes and the forces and moments have been obtained on both the nodes for different loading combinations. CAEPIPE does not show any results, which cause the failure of the piping system due to the forces and moments on the valves due to sustained and operating load cases. Following tables show the forces and moments on valves, which are coming due to operating and sustained load cases:

Node	Type	FX (lb)	FY (lb)	FZ (lb)	MX (ft-lb)	MY (ft-lb)	MZ (ft-lb)
40 50	Valve	-22372 22372	-10 15	0 0	0 0	0 0	3 8
80 90	Valve	13 -13	-3 9	0 0	0 0	0 0	-7 -3
130 140	Valve	-22372 22372	-12 17	0 0	0 0	0 0	8 5

Table 2.20: Valve forces: Operating Load

B. Sustained load case (L2)

Following table shows the forces and moments on valve nodes, which are coming due to sustained load. As clear from the sustained stress table 2.5, the stress ratios at all the valve nodes were less than 1, the valves are safe in the sustained load case.

Node	Type	FX (lb)	FY (lb)	FZ (lb)	MX (ft-lb)	MY (ft-lb)	MZ (ft-lb)
40	Valve	0	-4	0	0	0	2
50		0	9	0	0	0	3
80	Valve	11	-9	0	0	0	-1
90		-11	15	0	0	0	-8
130	Valve	0	-18	0	0	0	6
140		0	23	0	0	0	12

Table 2.21: Valve forces: Sustained Load

2.11.5 Expansion Load Case (L3 = T1)

2.11.5.1 Expansion Stresses: Following table shows the expansion stresses in the piping system. The stresses, which are marked red, are crossing the allowable limits. Thus indicating the failure of the piping system at corresponding nodes.

The stresses are high across the valves in between the nodes 40 to 50 and between nodes 130 and 140. The highest stress is found at node 145, at which the restraint in X direction has been put.

Expansion			
Node	SE (psi)	SA (psi)	SE / SA
145	46196	33312	1.39
115	45376	35989	1.26
140	45930	36739	1.25
55	45959	37779	1.22
130	45486	38514	1.18
30	45613	38903	1.17
50	45693	39194	1.17
40	45347	39414	1.15
150	31474	29739	1.06
60	31503	34514	0.91
20	859	35196	0.02
70	668	38237	0.02
80	573	39757	0.01
90	414	37729	0.01
110A	319	33509	0.01
100	318	36193	0.01
110B	193	33837	0.01
10	0	40106	0.00

Table 2.22: Expansion stresses

The figures below show the expansion stress distribution in the piping system.

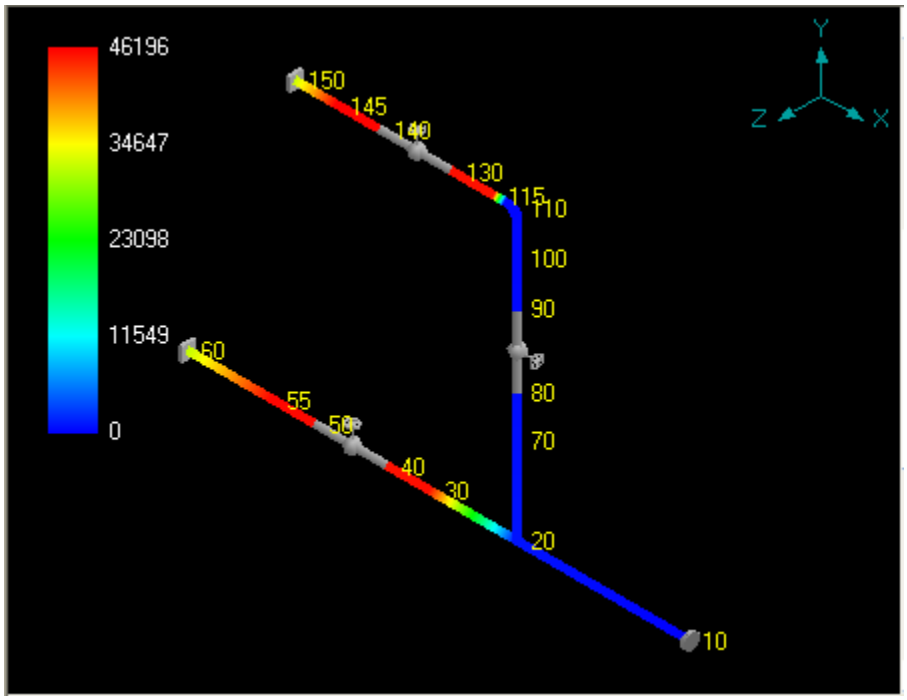

Fig 2.15: Expansion Stress Distribution in solid model

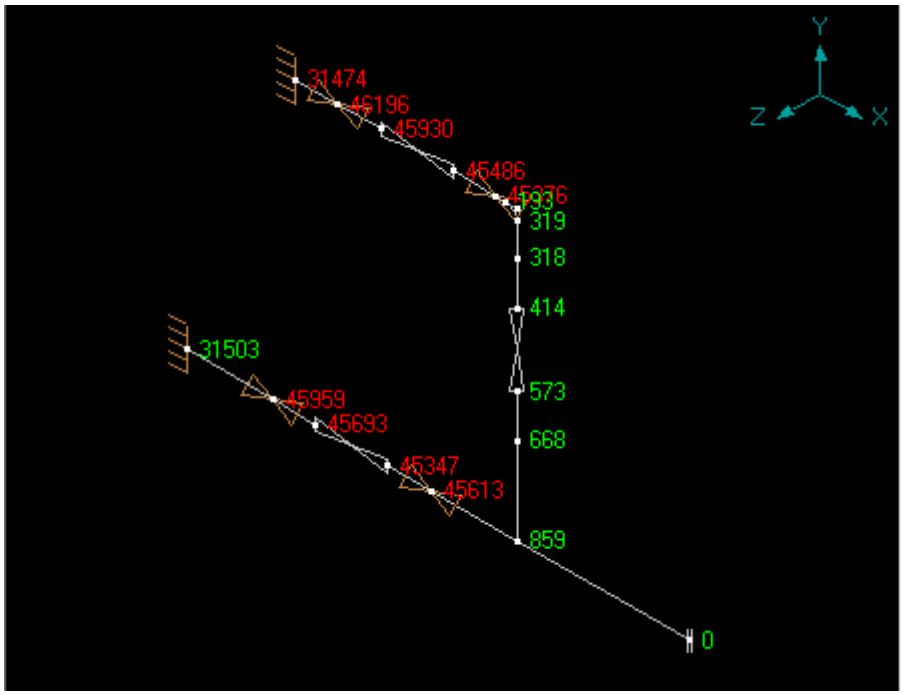

Fig 2.16: Expansion Stress Distribution in wire mesh model

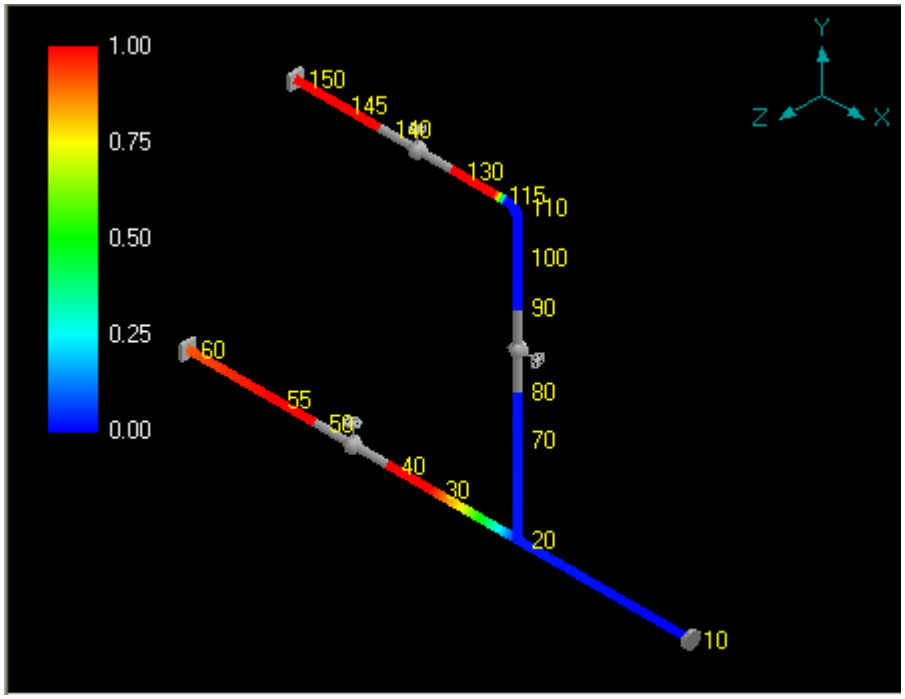

Fig 2.17: Expansion Stress ratios in solid model

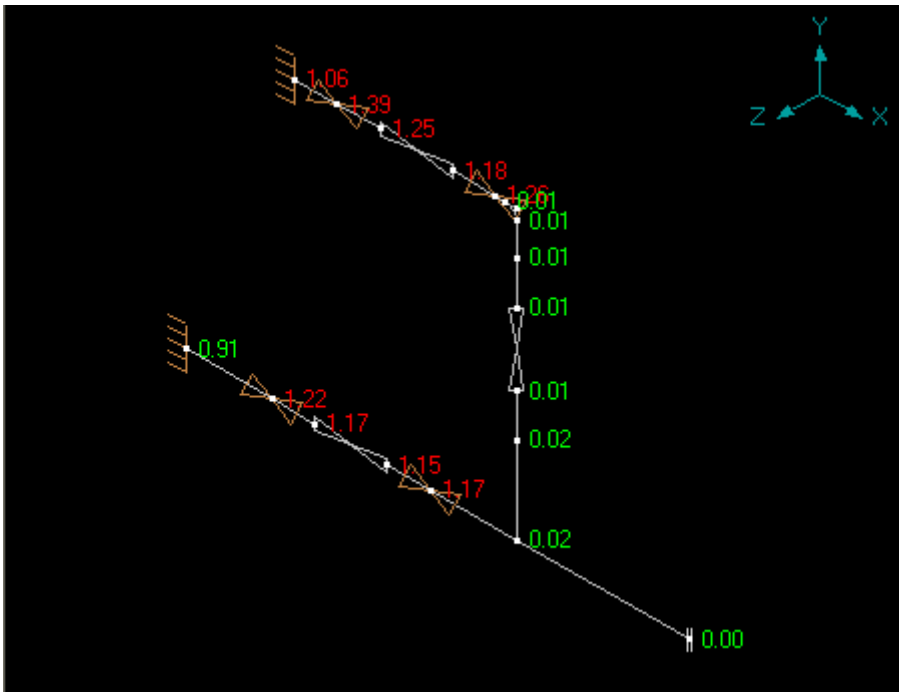

Fig 2.18: Expansion Stress ratios in wire mesh model

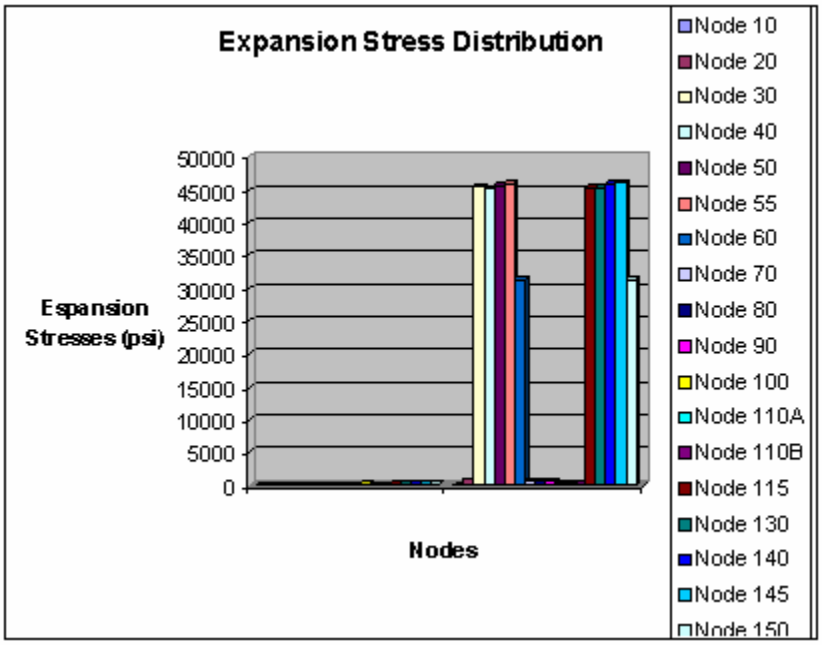

Fig 2.19: Expansion Stress distribution

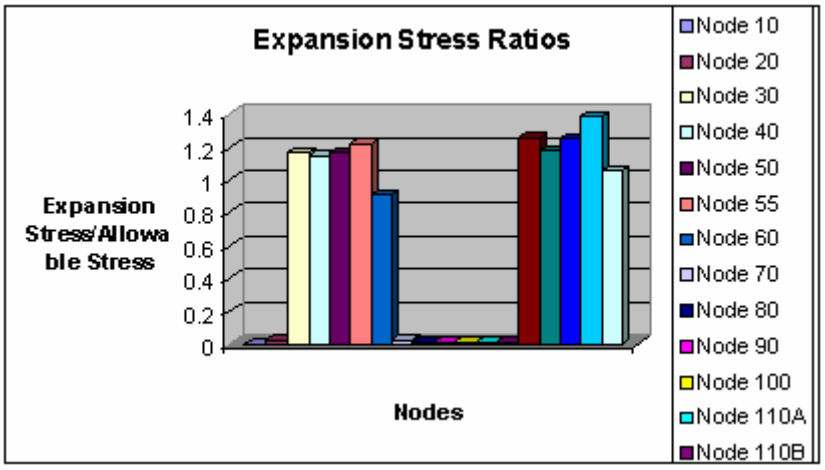

Fig 2.20: Expansion Stress ratios

2.11.5.2 Loads on Restraints: Expansion load case (T1)

Since all the restraints have been kept in X direction, the forces will be in the X-direction only. As clear from the table 2.22, the stress ratios at all the restraint nodes are more than1. The following table gives the magnitudes of the forces on the restraints due to expansion load case:

Node	FX (lb)	FY (lb)	FZ (lb)
30	22370		
55	-7402		
115	22374		
145	-7402		

Table 2.23: Restraints Loads: Expansion

2.11.5.3 Loads on Anchors: Expansion (T1)

The anchor at node 150 has stress ratio more than 1 as shown in table 2.22.

Node	FX (lb)	FY (lb)	FZ (lb)	MX (ft-lb)	MY (ft-lb)	MZ (ft-lb)
60	-14970	-6	0	0	0	-13
150	-14970	6	0	0	0	13

Table 2.24: Anchors Loads: Expansion

2.11.5.4 Pipe forces

As clear from the table 2.22, the expansion stresses at nodes 145, 115, 140, 55, 130, 30, 50, 40, 150 are higher than the corresponding allowable limits of expansion stresses. Thus the corresponding elements in the following tables are carrying the higher loads than the allowable

#	Node	FX (lb)	FY (lb)	FZ (lb)	MX (ft-lb)	MY (ft-lb)	MZ (ft-lb)
1	10 20	0 0	0 0	0 0	0 0	0 0	0 0
2	20 30	-2 2	-6 6	0 0	0 0	0 0	9 -3
3	30 40	-22372 22372	-6 6	0 0	0 0	0 0	3 -1
4	50 55	-22372 22372	-6 6	0 0	0 0	0 0	-4 7
5	55 60	-14970 14970	-6 6	0 0	0 0	0 0	-7 13
6	20 70	2 -2	6 -6	0 0	0 0	0 0	-9 7
7	70 80	2 -2	6 -6	0 0	0 0	0 0	-7 6
8	90 100	2 -2	6 -6	0 0	0 0	0 0	-4 3
9	100 110A	2 -2	6 -6	0 0	0 0	0 0	-3 3
10	110A 110B	2 -2	6 -6	0 0	0 0	0 0	-3 2
11	110B 115	2 -2	6 -6	0 0	0 0	0 0	-2 1
12	115 130	-22372 22372	6 -6	0 0	0 0	0 0	-1 -2
13	140 145	-22372 22372	6 -6	0 0	0 0	0 0	7 -10
14	145 150	-14970 14970	6 -6	0 0	0 0	0 0	10 -13

Table 2.25: Pipe forces – Expansion load

2.11.5.5 Element forces

Node	FX (lb)	FY (lb)	FZ (lb)	MX (ft-lb)	MY (ft-lb)	MZ (ft-lb)
10	0	0	0	0	0	0
20	0	0	0	0	0	0
20	-2	-6	0	0	0	9
30	2	6	0	0	0	-3
30	-22372	-6	0	0	0	3
40	22372	6	0	0	0	-1
40	-22372	-6	0	0	0	1
50	22372	6	0	0	0	4
50	-22372	-6	0	0	0	-4
55	22372	6	0	0	0	7
55	-14970	-6	0	0	0	-7
60	14970	6	0	0	0	13
20	2	6	0	0	0	-9
70	-2	-6	0	0	0	7
70	2	6	0	0	0	-7
80	-2	-6	0	0	0	6
80	2	6	0	0	0	-6
90	-2	-6	0	0	0	4
90	2	6	0	0	0	-4
100	-2	-6	0	0	0	3
100	2	6	0	0	0	-3
110A	-2	-6	0	0	0	3
110A	2	6	0	0	0	-3
110B	-2	-6	0	0	0	2
110B	2	6	0	0	0	-2
115	-2	-6	0	0	0	1

115 130	-22372 22372	6 -6	0 0	0 0	0 0	-1 -2
130 140	-22372 22372	6 -6	0 0	0 0	0 0	2 -7
140 145	-22372 22372	6 -6	0 0	0 0	0 0	7 -10
145 150	-14970 14970	6 -6	0 0	0 0	0 0	10 -13

Table 2.26: Element forces – Expansion load

2.11.5.6 Forces on Valve nodes

Valve forces are obtained by applying the expansion load cases on to the model. Valves have been assumed to connect to two nodes and the forces and moments have been obtained on both the nodes for expansion load case. CAEPIPE results show that the expansion stress at nodes 40, 50, 130 and 140 were more than the allowables, which cause the leakage of the piping system due to the forces and moments on the valves due to expansion load case. Following tables show the forces and moments on valves, which are coming due to expansion load case:

#	Node	Type	Fx (lb)	Fy (lb)	Fz (lb)	Mx (ft-lb)	My (ft-lb)	Mz (ft-lb)
1	40 50	Valve	-22372 22372	-6 6	0 0	0 0	0 0	1 4
2	80 90	Valve	2 -2	6 -6	0 0	0 0	0 0	-6 4
3	130 140	Valve	-22372 22372	6 -6	0 0	0 0	0 0	2 -7

Table 2.27: Valve forces – Expansion load

2.11.5.7 Effect of SIFs on expansion stresses in bend:

Following table gives the values of stresses in the bend with and without considering the SIFs:

Case	Node of Bend	SE
With SIF	110A	318
	110B	193
Without SIF	110A	247
	110B	148

Table 2.28: Effect of SIF on bend stress in expansion load case

It is clear from the table that the expansion stress values are higher while considering the SIFs. Thus by introducing SIFs the stresses are high as compared to the circumferential stresses so it prevents the initiation of the axial surface crack in the bend.

2.11.5.8 Displacements

Due to temperature gradient, expansion and contraction of pipe takes place, which will result in to displacement of system. Following table shows the value of maximum and minimum displacements of nodes in the piping system:

Direction	Type	Value	Node
X	Minimum	-0.003	50
(inch)	Maximum	0.039	10
Y	Minimum	-0.036	10
(inch)	Maximum	0.015	10
Z	Minimum	0.000	110B
(inch)	Maximum	0.000	10
XX	Minimum	0.000	10
(deg)	Maximum	0.000	10
YY	Minimum	0.000	10
(deg)	Maximum	0.000	10
ZZ	Minimum	-0.0449	40
(deg)	Maximum	0.0363	115

Table 2.29: Maximum and minimum displacements – Expansion load

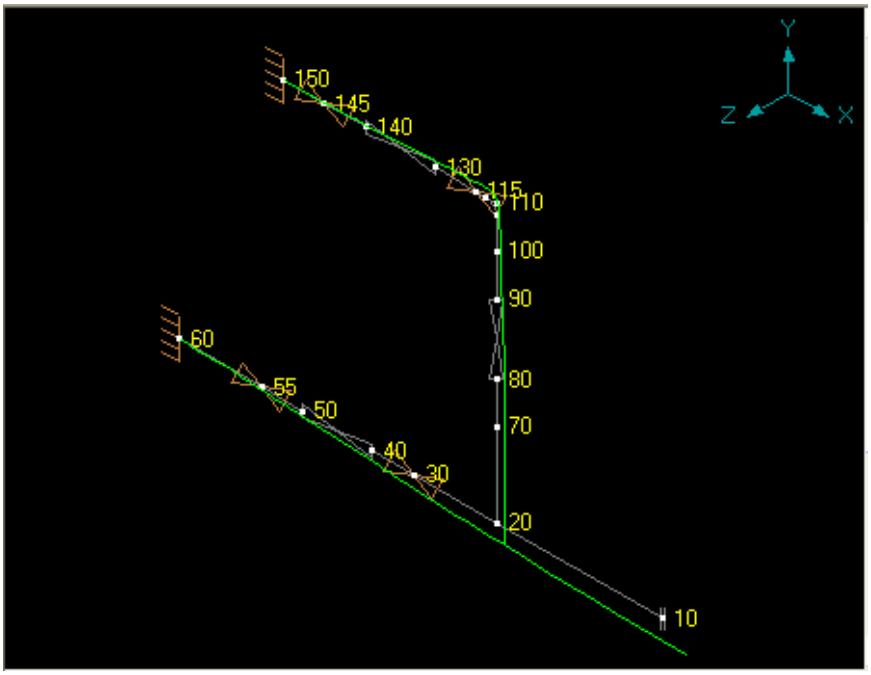

Fig 2.21: Deflected Shape due to Expansion load case (L3)

2.11.6 Effect of supports and restraints

Here in the modified model, the restraints at node 30, 55 and 115 has been removed. The new position of the restraints is at node 20, which is near to the flanged end, and at node 145.

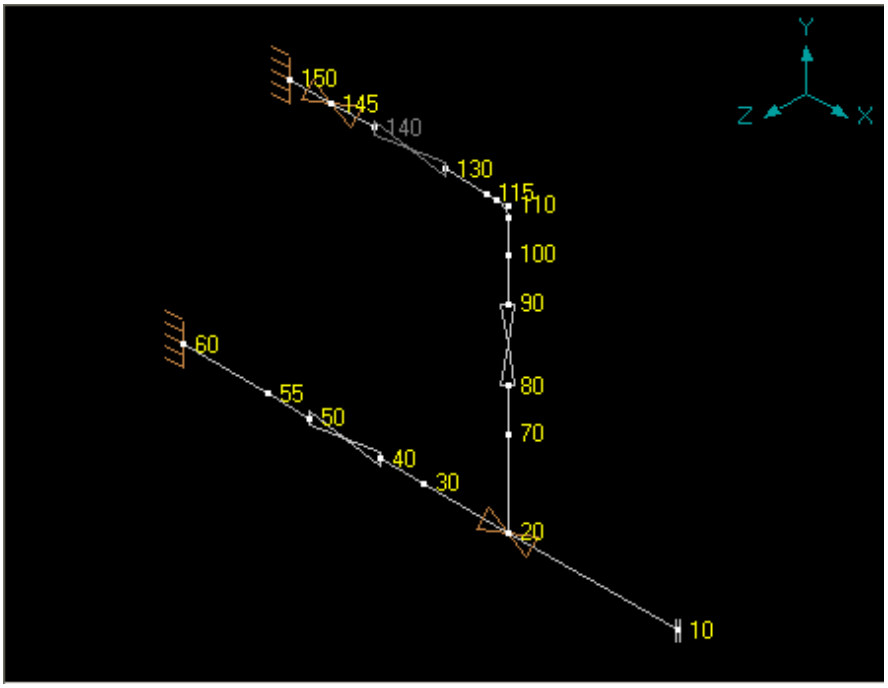

Fig 2.22: Modified model

Now the main purpose of the analysis with the modified model is to check the code stresses particularly the expansion stresses that were crossing the allowable limits in the original model. If percentage of code stress check is higher than 100%, then again the system will fail, whatever may be the nodal or restraint loads. As mentioned earlier, following are the load cases for the piping system under consideration:

1. L1 = W+T1+P1 (OPE)
2. L2 = W+P1 (SUS)
3. L3 = T1 (EXP)

For stress check, load cases L2 and L3 can be selected and for displacements and load check, load cases L1 and L2 can be selected.

Sustained Load Case (L2)

Original Model

#	Sustained			
	Node	SL (psi)	SH (psi)	SL/SH
1	150	12011	16700	0.72
2	145	8438	16700	0.51
3	110A	8218	16700	0.49
4	110B	7892	16700	0.47
5	60	7236	16700	0.43
6	20	6554	16700	0.39
7	115	5840	16700	0.35
8	100	5557	16700	0.33
9	140	5011	16700	0.30
10	90	4021	16700	0.24
11	55	3971	16700	0.24
12	70	3513	16700	0.21
13	130	3236	16700	0.19
14	30	2847	16700	0.17
15	50	2556	16700	0.15
16	40	2336	16700	0.14
17	80	1993	16700	0.12
18	10	1644	16700	0.10

Modified Model

#	Sustained			
	Node	SL (psi)	SH (psi)	SL/SH
1	150	12780	16700	0.77
2	145	9049	16700	0.54
3	110A	8833	16700	0.53
4	110B	8487	16700	0.51
5	60	7407	16700	0.44
6	20	7351	16700	0.44
7	115	6237	16700	0.37
8	100	5886	16700	0.35
9	140	5374	16700	0.32
10	90	4156	16700	0.25
11	55	4148	16700	0.25
12	70	3922	16700	0.23
13	130	3465	16700	0.21
14	50	2736	16700	0.16
15	30	2660	16700	0.16
16	80	2207	16700	0.13
17	40	2152	16700	0.13
18	10	1644	16700	0.10

Fig 2.23: Comparison of sustained stresses in original and modified model

The tables above show the stresses due to sustained load. As with the original model, the sustained stresses here also are within the allowable limits although the magnitude of the stresses has slightly changed as compared to the original model. Thus the code stresses for the sustained load case (L2) are in the safe limits.

2.11.6.1 Forces and Moments on Anchor at node 60

Load combination	FX (lb)	FY (lb)	FZ (lb)	MX (ft-lb)	MY (ft-lb)	MZ (ft-lb)
Sustained	0	-12	0	0	0	-20
Operating	-17784	-17	0	0	0	-35
Maximum	0	-12	0	0	0	-20
Minimum	-17784	-17	0	0	0	-35

With modified model

Load combination	FX (lb)	FY (lb)	FZ (lb)	MX (ft-lb)	MY (ft-lb)	MZ (ft-lb)
Sustained	0	-12	0	0	0	-19
Operating	-14970	-18	0	0	0	-33
Maximum	0	-12	0	0	0	-19
Minimum	-14970	-18	0	0	0	-33

With original model

Table 2.30: Comparison of load summary on anchor at node 60 in original and modified model

The forces due to operating load case (L1) on anchor at 60 have reduced with the changed boundary conditions. Also all the forces and moment are within the allowable limits due to both sustained and operating load conditions.

2.11.6.2 Forces and Moments on Anchor at node 150

Load combination	FX (lb)	FY (lb)	FZ (lb)	MX (ft-lb)	MY (ft-lb)	MZ (ft-lb)
Sustained	0	-27	0	0	0	-39
Operating	-14970	-22	0	0	0	-33
Maximum	0	-22	0	0	0	-33
Minimum	-14970	-27	0	0	0	-39

Modified model

Load Combination	FX (lb)	FY (lb)	FZ (lb)	MX (ft-lb)	MY (ft-lb)	MZ (ft-lb)
Sustained	0	-25	0	0	0	-36
Operating	-14970	-19	0	0	0	-23
Maximum	0	-19	0	0	0	-23
Minimum	-14970	-25	0	0	0	-36

Original model

Table 2.31: Comparison of load summary on anchor at node 150 in original and modified model

From the tables shown above, it is clear that there are no significant changes on the forces and moments on anchor at node 150. The loading on the anchor is within the safe limits.

2.11.6.3 Support load summary for restraint at node 145

Load combination	FX (lb)	FY (lb)	FZ (lb)
Sustained	0		
Operating	-7402		
Maximum	0		
Minimum	-7402		

Original model

Load combination	FX (lb)	FY (lb)	FZ (lb)
Sustained	12		
Operating	14980		
Maximum	14980		
Minimum	12		

Modified model

Table 2.32: Comparison of load summary on restraint at node 145 in original and modified model

From the above tables, it is clear that as the model has been modified, the loading on the restraints at node number 145 has rapidly increased. But CAEPIPE shows that the restraint is still in the safe limit.

2.11.6.4 Support load summary for restraint at node 20

Following table shows the forces on the restraint at node 20, which has been placed in the modified model.

Load combination	FX (lb)	FY (lb)	FZ (lb)
Sustained	-12		
Operating	17773		
Maximum	17773		
Minimum	-12		

Table 2.33: Support load summary for restraint at node 20

2.11.6.5 Minimum and maximum displacements during sustained load case (L2)

Direction	Type	Value	Node
X	Minimum	-0.002	100
(inch)	Maximum	0.002	70
Y	Minimum	-0.056	10
(inch)	Maximum	0.000	60
Z	Minimum	0.000	10
(inch)	Maximum	0.000	10
XX	Minimum	0.000	10
(deg)	Maximum	0.000	10
YY	Minimum	0.000	10
(deg)	Maximum	0.000	10
ZZ	Minimum	-0.081	130
(deg)	Maximum	0.0135	80

Original Model

Direction	Type	Value	Node
X	Minimum	-0.002	100
(inch)	Maximum	0.002	70
Y	Minimum	-0.065	10
(inch)	Maximum	0.000	60
Z	Minimum	0.000	10
(inch)	Maximum	0.000	10
XX	Minimum	0.000	10
(deg)	Maximum	0.000	10
YY	Minimum	0.000	10
(deg)	Maximum	0.000	10
ZZ	Minimum	-0.0862	130
(deg)	Maximum	0.0154	80

Modified model

Table 2.34: Comparison of Maximum and minimum displacements in original and modified model-Sustained load

The above two table show that there is negligible difference in the displacements in the original and modified model.

2.11.6.6 Minimum and maximum displacements during operating load case (L1)

The following tables give the values of maximum and minimum displacements in X, Y, Z directions in the original and modified model for the operating load case.

Direction	Type	Value	Node
X	Minimum	-0.003	50
(inch)	Maximum	0.039	10
Y	Minimum	-0.092	10
(inch)	Maximum	0.000	60
Z	Minimum	0.000	10
(inch)	Maximum	0.000	10
XX	Minimum	0.000	10
(deg)	Maximum	0.000	10
YY	Minimum	0.000	10
(deg)	Maximum	0.000	10
ZZ	Minimum	-0.0994	40
(deg)	Maximum	0.0333	90

Original model

Direction	Type	Value	Node
X	Minimum	-0.004	50
(inch)	Maximum	0.026	10
Y	Minimum	-0.129	10
(inch)	Maximum	0.000	60
Z	Minimum	0.000	10
(inch)	Maximum	0.000	10
XX	Minimum	0.000	10
(deg)	Maximum	0.000	10
YY	Minimum	0.000	10
(deg)	Maximum	0.000	10
ZZ	Minimum	-0.1396	10
(deg)	Maximum	0.000	60

Modified model

Table 2.35: Comparison of Maximum and minimum displacements in original and modified model-Operating load

2.11.6.7 Forces on valve nodes - operating load case (L1)

By comparing the results of forces and moments on valve nodes in the original and modified model, it is clear that the forces in X direction on valves on nodes 40-50 and nodes 130-140 have been significantly changed. Following table shows the forces and moments on valves, which are coming due to operating load:

Node	Type	FX (lb)	FY (lb)	FZ (lb)	MX (ft-lb)	MY (ft-lb)	MZ (ft-lb)
40	Valve	-22372	-10	0	0	0	3
50		22372	15	0	0	0	8
80	Valve	13	-3	0	0	0	-7
90		-13	9	0	0	0	-3
130	Valve	-22372	-12	0	0	0	8
140		22372	17	0	0	0	5

Original model

Node	Type	FX (lb)	FY (lb)	FZ (lb)	MX (ft-lb)	MY (ft-lb)	MZ (ft-lb)
40	Valve	-17784	-9	0	0	0	-2
50		17784	14	0	0	0	11
80	Valve	11	-6	0	0	0	-7
90		-11	11	0	0	0	-2
130	Valve	11	-15	0	0	0	2
140		-11	20	0	0	0	12

Modified model

Table 2.36: Comparison of Valve nodes forces in original and modified model – Operating load

2.11.6.8 Forces on valve nodes - sustained load case (L2)

By comparing the results of valve forces and moments in the original and modified model, it is clear that the forces in X direction on valves on nodes 40-50 and nodes 130-140 have been significantly changed. Following table shows the forces and moments on valves, which are coming due to operating load:

Node	Type	FX (lb)	FY (lb)	FZ (lb)	MX (ft-lb)	MY (ft-lb)	MZ (ft-lb)
40	Valve	0	-4	0	0	0	2
50		0	9	0	0	0	3
80	Valve	11	-9	0	0	0	-1
90		-11	15	0	0	0	-8
130	Valve	0	-18	0	0	0	6
140		0	23	0	0	0	12

Original model

Node	Type	FX (lb)	FY (lb)	FZ (lb)	MX (ft-lb)	MY (ft-lb)	MZ (ft-lb)
40	Valve	0	-4	0	0	0	2
50		0	9	0	0	0	4
80	Valve	12	-11	0	0	0	-2
90		-12	16	0	0	0	-8
130	Valve	12	-20	0	0	0	6
140		-12	25	0	0	0	13

Modified model

Table 2.37: Comparison of Valve nodes forces in original and modified model – Sustained load

2.11.6.9 Expansion Stresses: Load case L3

Original model

Expansion			
Node	SE (psi)	SA (psi)	SE/SA
145	46196	33312	1.39
115	45376	35989	1.26
140	45930	36739	1.25
55	45959	37779	1.22
130	45486	38514	1.18
30	45613	38903	1.17
50	45693	39194	1.17
40	45347	39414	1.15
150	31474	29739	1.06
60	31503	34514	0.91
20	859	35196	0.02
70	668	38237	0.02
80	573	39757	0.01
90	414	37729	0.01
110A	319	33509	0.01
100	318	36193	0.01
110B	193	33837	0.01
10	0	40106	0.00

Modified model

Expansion			
Node	SE (psi)	SA (psi)	SE/SA
60	37356	34343	1.09
150	30779	28970	1.06
55	36921	37602	0.98
20	36330	38509	0.94
50	36703	39014	0.94
145	30561	32790	0.93
30	36123	39090	0.92
40	36340	39598	0.92
110A	850	32917	0.03
110B	788	33263	0.02
100	616	35864	0.02
115	550	35513	0.02
90	566	37594	0.02
80	482	39543	0.01
70	432	37828	0.01
130	332	38285	0.01
140	35	36376	0.00
10	0	40106	0.00

Table 2.38: Comparison of Expansion stresses in original and modified model

The above two table show that the stresses due to expansion load case are reduced by a large amount in the modified model. The maximum stresses/allowable stress ratios are more than one only at nodes 60 and 150. Even the stresses at these nodes are only 6 to 9% higher than the allowable limits. In the original model the maximum value of SE/SA was 1.39 while in the modified model it has reduced to 1.09 only. The figures below show the stress distribution and stress ratios in the piping system for the expansion load case in the modified model.

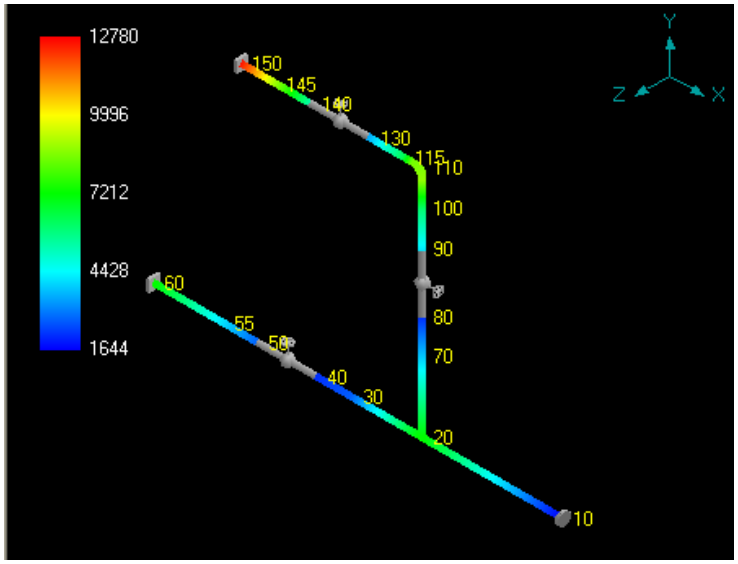

Fig 2.24: Expansion stress distribution in modified model

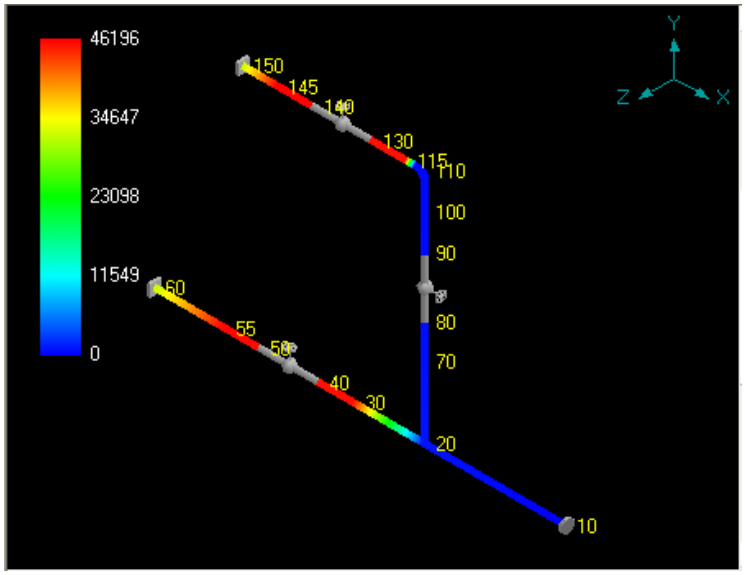

Fig 2.25: Expansion stress distribution in original model

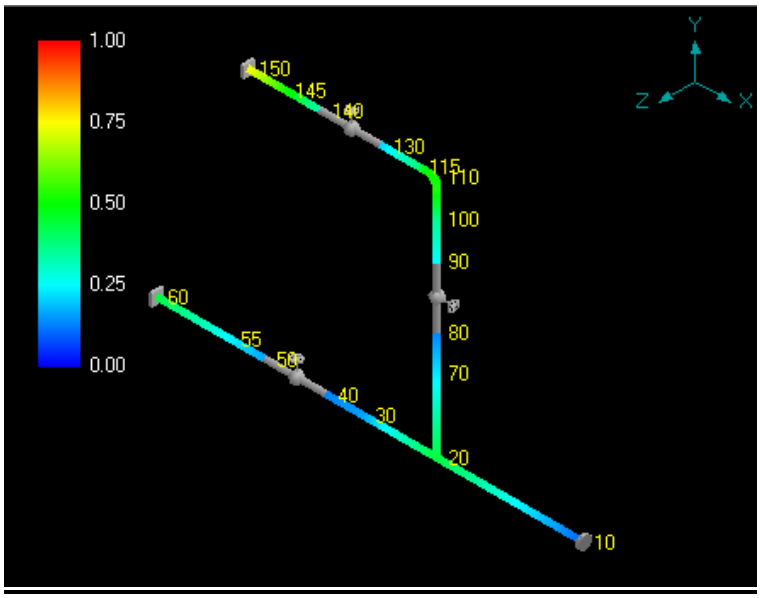

Fig 2.26: Expansion stress ratios in modified model

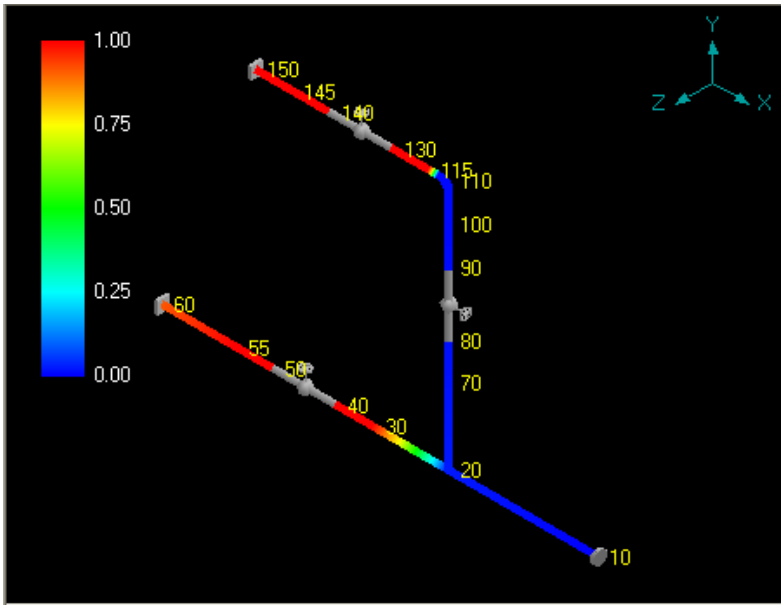

Fig 2.27: Expansion stress ratios in original model

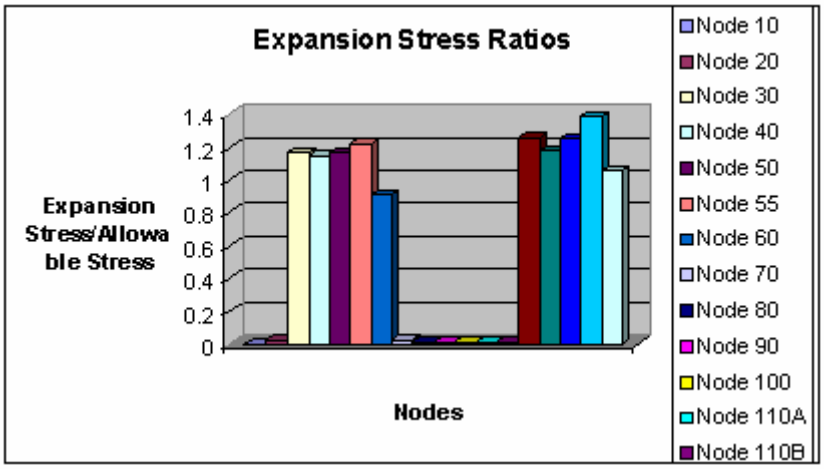

Fig 2.28: Expansion stress ratios in original model-Graph

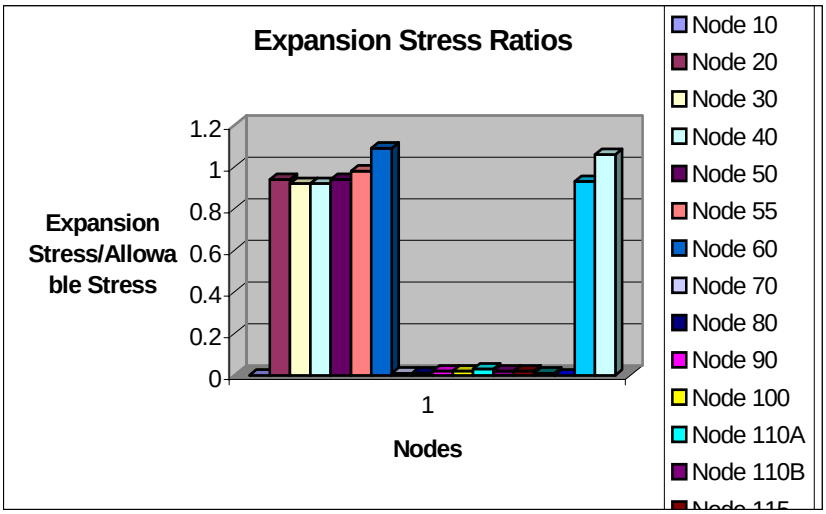

Fig 2.29: Expansion stress ratios in modified model-Graph

2.11.7 Conclusion

The purpose of the static analysis was to check nodal loads, support loads (restraints and anchors), loads on valves and element forces and to check the code stresses (Sustained and Expansion stresses). By having a look at the results it is clear that the system is going to fail due to expansion stresses at nodes 145, 115, 140, 55, 130, 30, 50, 40, and 150, as the ratio of Maximum stress/Allowable stress is more than 1 for these nodes. CAEPIPE results show the expansion stresses at these nodes in the red color, which indicates that these stresses are crossing the allowable limits. Therefore after getting the results of static analysis, the primary objective was to reduce the stresses on these nodes so that these stresses can come within the allowable limits.

CAEPIPE results show that the system is going to fail only due to these expansion stresses and all the other results are within the allowable limits. The displacements, the loads on anchors, restraints, valves and nodes due to all the three possible load cases operating, sustained and expansion are safe for the piping system. After removing the restraints from nodes 30, 55 and 115 and putting a new restraint near to the flanged end at node number 20, the expansion stresses are reduced in most part of the piping system. The new modified model is also safe for the sustained stresses, support and restraint loadings, valve forces, displacements of nodes etc. in all the three load cases.

Chapter 3

Transient Flow Analysis

3.1 Introduction

Pressure waves in piping result from changes in the fluid velocity. Their amount depends on the extent of fluid acceleration or deceleration and on the fluid density as well as the local sound velocity. These pressure waves, which run through the piping, cause transient forces on the piping system, the extent of which shows the same dependence, whereas their effect is notably influenced by the pipe geometry. Rapid changes in the velocity of a flowing fluid lead to simultaneous pressure changes, which propagate, from the point of velocity change with the local sound velocity of the fluid into the piping system. These pressure waves are reflected in different ways at ends, branches or cross–section changes. They combine and apparently run randomly to and fro in the piping until they die out after a certain time as a result of damping.

3.2 Water hammer

This chapter deals with the water hammer induced transient flow analysis. The main focus is to analyze the effect of suddenly stopping or accelerating a fluid by closing or opening of the valves. The effect of closing the different valves at different times was analyzed as a special parameter to control the maximum pressure.

Water hammer is a phenomenon that occurs in all piping systems whenever some event disturbs the steady state. Rapid disturbances cause large transient pressures that in extreme cases can cause a catastrophic failure of the piping system and/or damage to associated equipment. Regardless of the magnitude, water hammer always exists when the liquid velocity in a piping system is changed. The disturbances consist of coupled pressure and velocity waves that propagate throughout a piping system. The wave speed can be calculated as from the following equation:

$$a = \frac{12}{\left[\frac{w}{g}\left(\frac{1}{K} + \frac{d}{Et}\right)\right]^{1/2}}$$

$$a = 440.016\, ft/\sec$$

Where, a = wave velocity, ft/s

w = specific weight of fluid lb/ft3

K = Bulk modulus of compressibility of liquid, psi

E = Modulus of elasticity of pipe wall, psi

d = Inside diameter of pipe, in

t = Pipe wall thickness, in

g = Acceleration due to gravity, ft/s^2

Water hammer pressure surges can be calculated using the Talbot formula as follows:

$$\Delta P = \frac{aWV}{144g}$$

$$\Delta P = 0.68\, psi$$

Where, ΔP = Pressure above normal, psig.

3.3 Assumptions

It has been assumed that the upstream supply is a reservoir, which acts as a fixed pressure. Thus the pressure remains constant at the inlet. The figure below shows the schematic of the model:

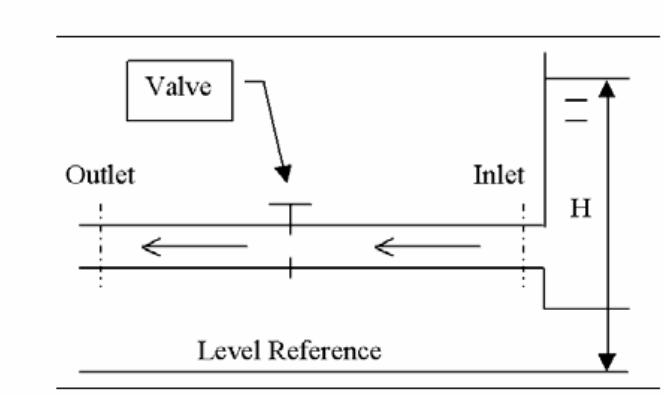

Fig 3.1: Transient flow model

3.4 Valve closure time and reflection period

Transient events communicate their effect through the pipe at the wave speed. When transient events occur, they are communicated upstream (or downstream) so the system can adjust to the new conditions. No response to the changing conditions can be obtained until the communication wave travels to the other end of the pipe and back. When the valve closes, this fact is communicated up the pipe to the supply, telling it to stop supplying fluid because fluid is no longer needed. This communication takes a finite time, and this time is in fact related to the wave speed. The communication will complete a full cycle after the response reflects back to the valve. The total time, which the pressure wave takes for traveling from valve to the upstream supply and then after reflecting from upstream supply to the valve, is called as the reflection period of the pipe, T_R. The following relation gives this reflection period:

$$T_R = \frac{2L}{a}$$

Where, L is the length of the pipe, upstream, ft

a = Pressure wave speed, ft/s.

Maximum surge pressure results when the time required to change a flow velocity a given amount is equal to or less than:

$$\tau \leq T_R$$

Where, τ is valve closure time. Lower the valve closure time, i.e. rapid the valve closure, higher will be the value of pressure surge.

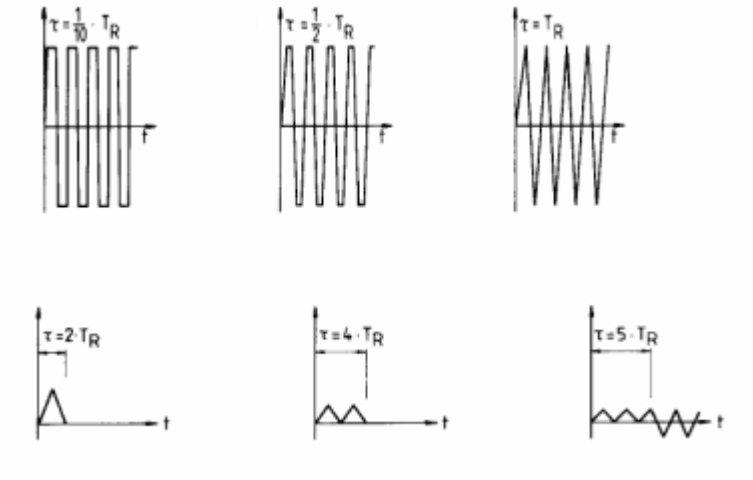

Fig 3.2: Effect of valve closing period on pressure

3.5 Flow rate variations

The flow rate varies with the time as per the relationship given by:

$$Q(t) = Q_0(1 - \frac{t}{\tau}) \; for (0 \le t \le \tau)$$
$$Q(t) = 0 \; for (t > \tau)$$

Following figures shows the variations of flow rates with time for different valves. As clear from the graphs, the flow rate becomes zero once the valve reaches to the respective valve closure times.

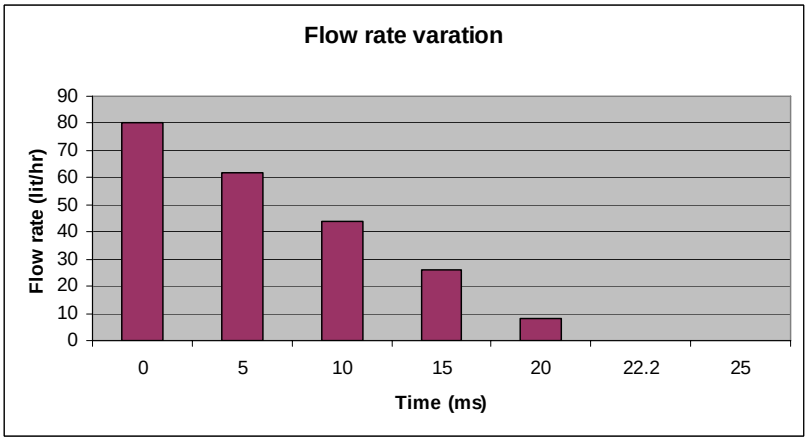

Fig 3.3: Flow rate variation for valve at node 40-50.

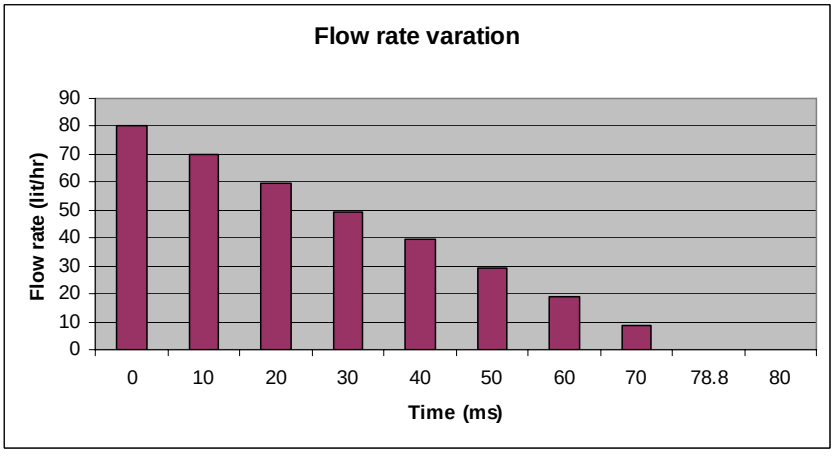

Fig 3.4: Flow rate variation for valve at node 80-90.

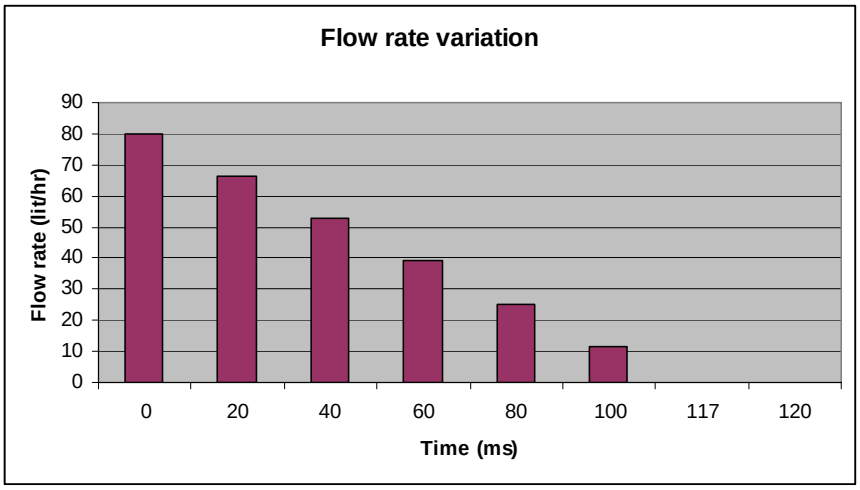

Fig 3.5: Flow rate variation for valve at node 130-140.

3.6 Results and discussion

CAEPIPE uses force spectrum analysis option to determine the response of the piping system to sudden impulsive load due to water hammer. In force spectrum analysis, the results of the modal analysis are used to determine the response of the piping system. CAEPIPE defines the time functions for valves for different valve closing times and then converts it into force spectrums.

3.6.1 Dynamic stresses due to water hammer effect

CAEPIPE calculates the stresses developed due to water hammer at different nodes. It has been assumed that at a time only one valve is closed. Thus the software calculates the dynamic stresses for closing of different valves separately. Following tables and figures shows the stress values for different valve closures.

Occasional			
Node	SL+SO (psi)	1.33SH (psi)	SL+SO / 1.33SH
150	12011	22211	0.54
145	8438	22211	0.38
110A	8241	22211	0.37
110B	7913	22211	0.36
60	7236	22211	0.33
20	6554	22211	0.30
115	5840	22211	0.26
100	5557	22211	0.25
140	5011	22211	0.23
90	4021	22211	0.18
55	3971	22211	0.18
70	3513	22211	0.16
130	3236	22211	0.15
30	2847	22211	0.13
50	2556	22211	0.12
40	2336	22211	0.11
80	1993	22211	0.09
10	1644	22211	0.07

Table 3.1: Occassional stresses when Valve between nodes 40 and 50 is closed

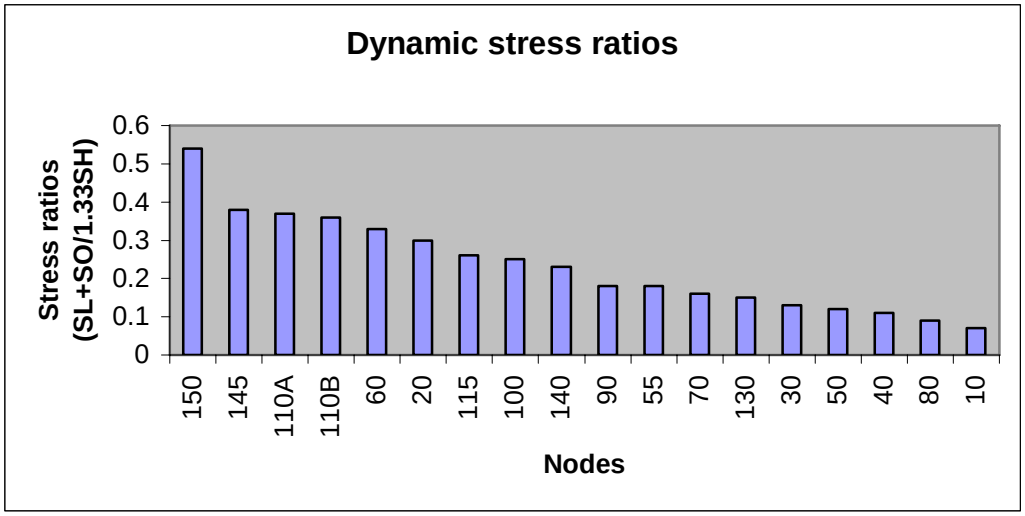

Fig 3.6: Dynamic stress ratios when Valve between nodes 40 and 50 is closed

.

Occasional			
Node	SL+SO (psi)	1.33SH (psi)	SL+SO / 1.33SH
150	20636	22211	0.93
20	17861	22211	0.80
60	16206	22211	0.73
145	14402	22211	0.65
110A	12543	22211	0.56
110B	11790	22211	0.53
30	9754	22211	0.44
100	8824	22211	0.40
115	8414	22211	0.38
140	8341	22211	0.38
70	8263	22211	0.37
40	7806	22211	0.35
90	7605	22211	0.34
80	6386	22211	0.29
55	6307	22211	0.28
130	4037	22211	0.18
50	4003	22211	0.18
10	1644	22211	0.07

Table 3.2: Occassional stresses when Valve between nodes 80 and 90 is closed

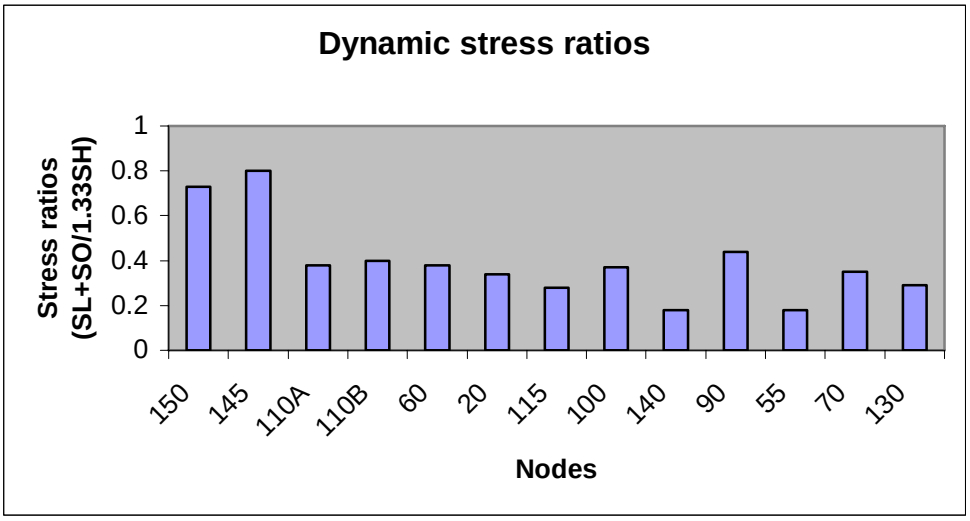

Fig 3.7: Dynamic stress ratios when Valve between nodes 80 and 90 is closed

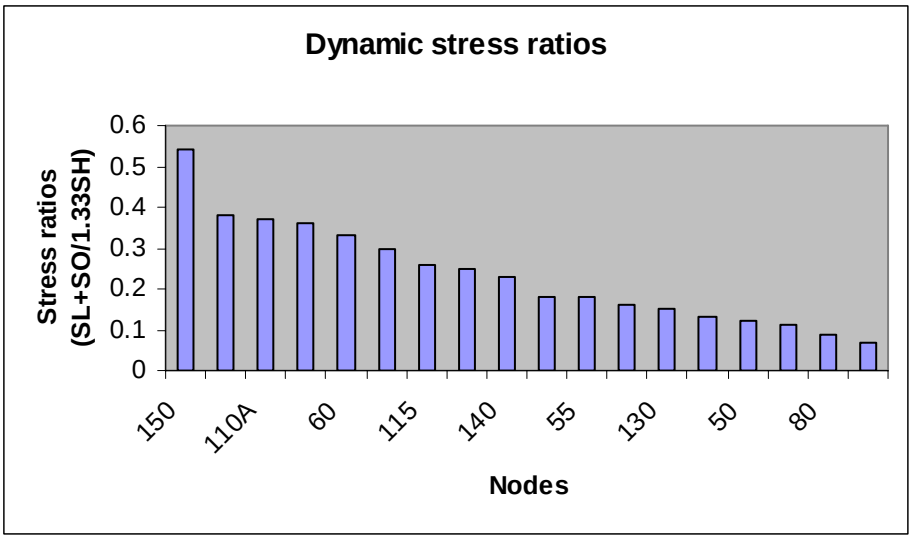

Fig 3.8: Dynamic stress ratios when Valve between nodes 130 and 140 is closed

3.6.2 Variation of pressure with valve closure times

The pressure in the piping system varies with the valve closure time according to the following relationship:

$$P = \frac{0.07VL}{\tau} + P_i$$

Thus the following graphs are obtained for the pressure variation:

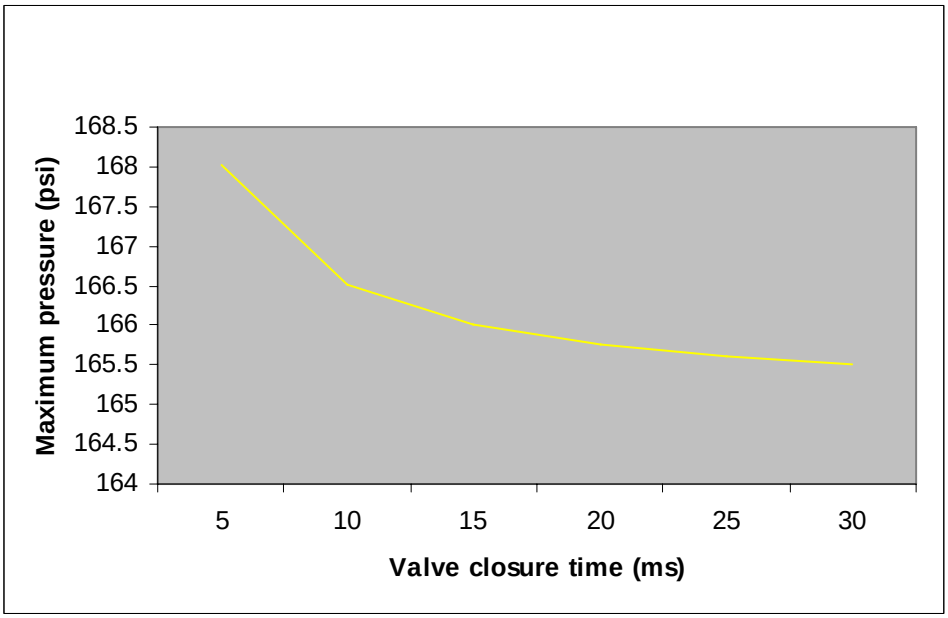

Fig 3.9: Pressure variation for valve between nodes 40-50.

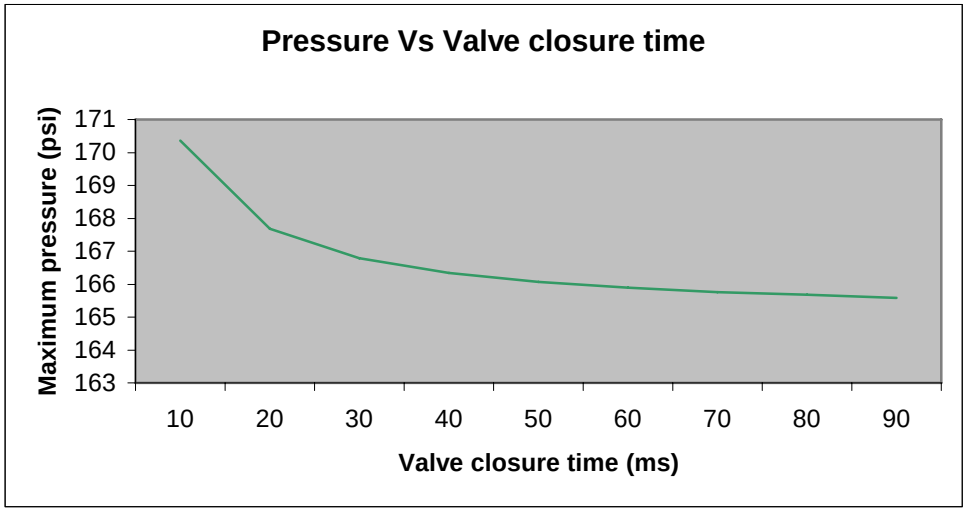

Fig 3.10: Pressure variation for valve between nodes 80-90.

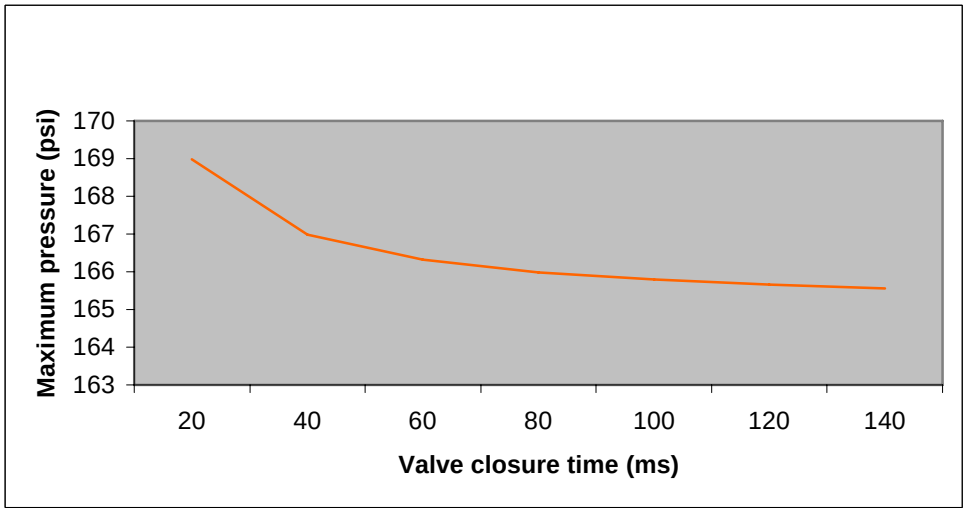

Fig 3.11: Pressure variation for valve between nodes 130-140.

3.6.3 Reflection periods

Reflection periods for different sections of the piping system can be found out as follows:

(i) Between node 50 and 60

$$T_{R_{50-60}} = \frac{2L_{50-60}}{a}$$

$$T_{R_{50-60}} = 6.81ms$$

(ii) Between node 60 and 80

$$T_{R_{60-80}} = \frac{2L_{60-80}}{a}$$
$$T_{R_{60-80}} = 24.22ms$$

(iii) Between node 60 and 130

$$T_{R_{60-130}} = \frac{2L_{60-130}}{a}$$
$$T_{R_{60-130}} = 35.95ms$$

3.6.4 Valve closing times

(i) Valve between nodes 40 and 50

$$\tau_{40-50} = \frac{0.07VL_{50-60}}{P - P_i}$$
$$\tau_{40-50} = 22.2ms$$

(ii) Valve between nodes 80 and 90

$$\tau_{80-90} = \frac{0.07VL_{60-80}}{P - P_i}$$
$$\tau_{80-90} = 78.8ms$$

(iii) Valve between nodes 130 and 140

$$\tau_{130-140} = \frac{0.07VL_{60-130}}{P - P_i}$$
$$\tau_{130-140} = 117ms$$

3.6.5 Unbalanced load

The magnitude of the unbalanced load can be calculated as follows:

$$F_{unbalanced} = \Delta P \times A_i$$
$$F_{unbalanced} = 0.68\,psi \times \frac{\pi}{4} \times d_i^{\,2}$$
$$F_{unbalanced} = 0.68 \times \frac{\pi}{4} \times 1.049^2 = 0.5876lbf = 2.6442N$$

3.7 Conclusion

The results show that the stresses due to transient loads (water hammer) are all within the allowable limits. For different valves closure, stresses were found out. The piping system is safe from these stresses. Also the graphs for the dynamic stress ratios were plotted. Valve closure times have been calculated along with the reflection periods. For minimizing the pressure surges the valve closure times must be higher than the reflection periods and results show that for all the valves, the valve closure time is higher as compared to the reflection period. Graphs have been plotted for all the valves, which show the reduction of maximum pressure with the increase in time of the valve closing.

Chapter 4
Summary and Conclusions

4.1 Summary

The study under this thesis work covers the static, thermal and transient flow analysis of a piping system. The study considers the static, thermal and dynamic stresses due to water hammer effect. In the static analysis, the stresses, displacements, support forces and moments and element forces and moments were obtained. Results obtained from the software show that the piping system is safe in static analysis.

In the thermal analysis also the stresses, displacements, support forces and moments and element forces and moments were obtained. The results of thermal analysis show that system was getting failed due to excessive thermal stresses at various nodes. The ratio of maximum expansion stress to allowable stress were more than1 at nodes 145,115,140, 55, 130, 30, 50 40 and 150. For solving this problem, some modification in the model were done by removing the restraints at nodes 30, 55 and 115 and by putting a new restraint near to the flanged end at node 20. And comparisons were made between the results of original and modified model for stresses, displacements, element forces and support forces and moments. Due to the modification most of the nodes, which were crossing the allowable limits, came within the limits.

In the water hammer analysis of the piping system, dynamic stresses were found out for the closing of different valves separately. Also the valve closure times for the valves and the reflection periods of the different sections were found out. Graphs were obtained for pressure variation with the valve closure times for the valves. The results show that the system is under no threat due to the water hammer effect.

4.2 Conclusions

In the structural analysis of the piping system, all the stresses at various nodes of the system due to sustained load and operating load cases were obtained and the highest value of ratio of maximum stress to allowable stress was found at node 150 (0.72) for

sustained load case. Thus the piping system was found to be safe for operating and sustained load cases.

In the thermal analysis of the piping system, the stress ratios were found to be more than 1 at nodes 145,115,140, 55, 130, 30, 50 40 and 150. The highest value of the ratio of maximum stress to allowable stress was found at node 145 (1.39). After the modification of the model most of these nodes came in to the allowable limits. In the modified model only two nodes (node 60 and node 150) were crossing the allowable nodes but the highest value of ratio of maximum stress to allowable stress was reduced to 1.09 at node 60.

In the water hammer analysis of the piping system dynamic stresses were obtained due to sudden closing of different valves separately. The wave speed was calculated as 440.016 ft/sec and the pressure surge was 0.68 psi. For sudden closing of the valve at node 40-50, the highest value of ratio of the maximum stress to the allowable stress was found to be at node 150 (0.54). Thus the pressure wave was not creating any significant effect on the piping system due to sudden closing of valve. For sudden closing of the valve at node 80-90 the highest value of ratio of the maximum stress to the allowable stress was also found to be at node 150 (0.93). Thus in this case also the system was safe. And for the sudden closing of the valve at node 130-140 also the highest ratio of maximum stress to allowable stress was found to be at node 150 and same as for the valve at node 40-50 i.e. 0.54. Thus the system was considered safe for the water hammer induced fluid pressure waves. The valve closure time for valve at node 40-50 was found as 22.2 ms, for valve at node 80-90 it is 78.8 ms and for the valve at node 130-140 the value of valve closure time is 117 ms. The reflection period for the pipe between node 50-60 is 6.81 ms, for the pipe between 60-80 its value is 24.22 ms and for the pipe between node 60-130 its value is 35.95 ms. Thus by comparing the valve closure times for different valves with the corresponding reflection period it was found out that for all the valves the valve closure times were greater than the reflection periods. Thus fulfilling the condition of reducing the pressure surge to prevent the piping system from the failure due to water hammer effect. The following table shows this:

Node	Type	Valve closure time τ , (ms)	Pipe length for calculating reflection, period between node	Reflection period T_R, (ms)	Is $T_R \leq \tau$
40-50	Valve	22.2	50-60	6.81	Yes
80-90	Valve	78.8	60-80	24.22	Yes
130-140	Valve	117	60-130	35.95	Yes

Table 4.1: Reflection periods and valve closing times

4.3 Future Work

The stresses due to expansion load cases were although reduced by a significant amount but still at nodes 60 and 150 the stresses were little bit more than allowable limits. These stresses have to be reduced. The model can be analyzed for the temperature change throughout the wall of the pipe. Also for dynamic analysis, velocity was assumed constant but it may change due to friction and other obstacles in the system. The model can be analyzed for the creep loading also.

References

1. “Numerical fluid-hammer analysis by the method of characteristics in complex piping networks.” By Yong W. Shin and William L Chen, Nuclear Engineering and Design, Volume 33, Issue 3, September 1975, Pages 357-369
2. “Pipe rupture and steam/water hammer design loads for dynamic analysis of piping systems.” By Benjamin R. Strong, Jr. and Ronald J. Baschiere, Nuclear Engineering and Design, Volume 45, Issue 2, February 1978, Pages 419-428
3. “Water Hammer Production and Design Measures in Piping Systems.” By R. Gillessen & H. Lange, International Journal of Pressure Vessels and Piping, Volume 33, Issue 3, 1988, Pages 219-234
4. “Structural dynamics and fracture mechanics calculations of the behavior of a DN 425 test piping system subjected to transient loading by water hammer.” By K. Kussmaul, E. Kobes, H. Diem, D. Schrammel and S. Brosi, Nuclear Engineering and Design, Volume 151, Issues 2-3, 2 November 1994, Pages 473-487
5. “Elastic-plastic water hammer analysis in piping systems.” By A.Khamlichi, L. Jezequel and F. Tephany, Wave Motion, Volume 22, Issue 3, November 1995, Pages 279-295.
6. “Validation of Hyperbolic Model for Water-Hammer in Deformable Pipes.” By E. Hadj Taieb and T. Lili, Journal of fluids Engineering, March 2000,Volume 122, Issue1, pp. 57-64
7. “Span Limits for Elevated Temperature Piping.” By Charles Becht IV and Yaofeng Chen Journal of Pressure Vessel Technology, May 2000, Volume 122, Issue 2, pp. 121-124
8. “Creep Relaxation Behavior of High-Energy Piping.” By Raymond K. Yee and Marvin J. Kohn, Journal of Pressure Vessel Technology, November 2000, Volume 122, Issue 4, pp. 488-493
9. “Mechanical Behavior of a Branch Pipe Subjected to Out-of-Plane Bending Load.” By S. Chapuliot, D. Moulin and D. Plancq, journal of Pressure Vessel Technology, February 2002, Volume 124, Issue 1, pp. 7-13

10. “Models for analysis of water hammer in piping with entrapped air.” By M.A. Chaiko and K.W. Brinkman, Journal of Fluids Engineering, March 2002, Volume 124, Issue 1, pp. 194-204
11. “Nonlinear Response and Failure of Steel Elbows Under In-Plane Bending and Pressure.” By S. A. Karamanos, E. Giakoumatos and A. M. Gresnigt, Journal of Pressure Vessel Technology, November 2003, Volume 125, Issue 4, pp. 393-402.
12. “Nonlinear response and failure of steel elbows under in-plane bending and pressure.” By S.A. Karamanos, E. Giakoumatos and A.M. Gresnight, Journal of Pressure Vessel Technology -- November 2003 -- Volume 125, Issue 4, pp. 393-402
13. “A new finite element formulation based on the velocity of flow for water hammer problems.” By Jayaraj Kochupillai, N. Ganesan, Chandramouli Padmanabhan, International Journal of Pressure Vessels and Piping, Volume 82, Issue 1, January 2005, Pages 1-14
14. “The thermal and mechanical behavior of structural steel piping systems.” By E.M.M. Fonseca, F.J.M.Q. de Melo, C.A.M. Oliveira, International Journal of Pressure Vessels and Piping, Volume 82, Issue 2, February 2005, Pages 145-153
15. “Two dimensional pipe model for laminar flow.” By M. C. P. Brunelli, Journal of Fluids Engineering -- May 2005 -- Volume 127, Issue 3, pp. 431-437
16. “Effect of loading on stress intensification factors.” By Rudolph J. Scavuzzo, Jr., Journal of Pressure Vessel Technology, February 2006, Volume 128, Issue 1, pp. 33-38
17. ASME B 31.3 for Process Piping-2002 edition.
18. “Piping Handbook by Crocker and King” Fifth Edition, McGraw-Hill, pp.3-189 to 192, 1980.
19. “Design of piping system.”, John Willey & Sons, 2nd edition.
20. “Piping design for process plants.” By Howard F. Rase, Robert E. Krieger publishing company, Malabar, Florida.

21. “Handbook of Industrial pipe work engineering.” By Holmes.
22. “Piping stress handbook.” By Victor Helgnero M. 1983.
23. “Piping calculation manual.” By Menon and E. Shashi.
24. A book on piping engineering course by IITB.

Appendices

Appendix A

Model Layout

Table below gives the layout geometry of the piping system model.

#	Node	Type	DX(ft'in")	DY(ft'in")	DZ(ft'in")	Matl	Sect	Load	Data
1	10	From							Flange
2	20		-2'0"			1	1	1	
3	30		-1'0"			1	1	1	X restraint
4	40		-0'6"			1	1	1	
5	50	Valve	-0'10"			1	1	1	
6	55		-0'6"			1	1	1	X restraint
7	60		-1'0"			1	1	1	Anchor
8	20	From							
9	70			1'0"		1	1	1	
10	80			0'6"		1	1	1	
11	90	Valve		0'10"		1	1	1	
12	100			0'6"		1	1	1	
13	110	Bend		0'6"		1	1	1	
14	115		-0'3"			1	1	1	X restraint
15	130		-0'6"			1	1	1	
16	140	Valve	-0'10"			1	1	1	
17	145		-0'6"			1	1	1	X restraint
18	150		-0'6"			1	1	1	Anchor

Note:

1. Load 1 is defined as 165 psi pressure and 85 degree centigrade temperature.
2. Material 1 is defined as ASTM A 312 TP304L.
3. Section 1 is defined as 1" NPS pipe with thickness as schedule 40S (0.133").

Appendix B

Tables for elements and data

1. Anchors (2)

Node	KX (lb/inch)	KY (lb/inch)	KZ (lb/inch)	KXX (in-lb/deg)	KYY (in-lb/deg)	KZZ (in-lb/deg)
60	Rigid	Rigid	Rigid	Rigid	Rigid	Rigid
150	Rigid	Rigid	Rigid	Rigid	Rigid	Rigid

2. Bends (1)

Bend Node	Radius (inch)	Radius Type	Bend Material
110	1.5	Long	1

3. Restraints (4)

Node	X	Y	Z
30	Y		
55	Y		
115	Y		
145	Y		

4. Ball Valves (3)

From	To	Weight (Kg)	Length (inch)
40	50	2.268	10
80	90	2.268	10
130	140	2.268	10

Appendix C

CAEPIPE Features

1. **Modeling:** CAEPIPE provides easy model generation and powerful editing feature. Various elements which can be input to the piping system model are pipe, elbow/bend (flexibility factor, user SIF, different material, thickness etc.), miter bend, jacketed bend and pipe, reducer, rigid element, valve, bellows, slip joint, hinge joint, ball joint, beam and elastic element. It also provides various support types like rigid and flexible anchor, two-way rigid restraint, guide and hangers, limit stop. Other useful data are flange, force and moment, spider, nozzle, weld, concentrated mass and SIFs. It provides various built-in databases like pipe sizes (ANSI, JIS and DIN), material libraries, valve library and flange library.

2. **Analysis:** Analysis features include static linear/non-linear analysis for sustained, expansion, operating, occasional load cases. Various load combinations can be input to the piping system models like weight and multiple pressures, external forces and moments, combination of pressure, weight and temperature, time history loads, harmonic loads. Thermal case is solved by taking the difference between the results of operating and sustained load case.

3. **Results:** As an output one can get the displacements, minimum and maximum displacements for each load case, deflected shape with animation, support loads for all load cases, element forces and moments, code compliance stresses, plotted stresses and stress ratios, rotating equipment reports, frequencies and mode shapes, color coded stresses and stress ratios and center of gravity calculation.

4. **Import and export:** CAEPIPE imports data from CADCentre PDMS, Intergraph PDS, PIPESTRESS, CAEFLOW, CAEPIPE batch file and exports data to AutoCAD DXF, PIPESTRESS, CAEFLOW, CAEPIPE batch file, Microsoft Excel CSV file (materials, spectrums, time functions, time-history results.)